Vol. 53: 205–227, 2012
doi: 10.3354/cr01095

CLIMATE RESEARCH
Clim Res

Published July 19

Wintertime circulation types over the Iberian Peninsula: long-term variability and relationships with weather extremes

S. Fernández-Montes[1,*], S. Seubert[2], F. S. Rodrigo[1], E. Hertig[2]

[1]Department of Applied Physics, University of Almería, La Cañada de San Urbano, s/n, 04120 Almería, Spain
[2]Institute of Geography, University of Augsburg, Universitätsstrasse 10, 86135 Augsburg, Germany

ABSTRACT: This paper analyses atmospheric surface circulation and climatic extremes in the Iberian Peninsula in winter (December–February). Sea level pressure grids (1850–2003) are classified through a simulated annealing clustering into 7 characteristic circulation types (CTs). Daily series of temperature (29 stations) and precipitation (44 stations) started between 1905 and 1950. We investigate which CTs are conducive to extremes at each station by means of their contribution to extreme days compared to non-extremes days, with significance based on a Monte Carlo resampling. Regional features arise in the relationship between CTs and extremes and, taking them into account, some trends in extreme indices from 1950–2003 (period shared by all stations) agree with trends in the frequency of the CTs. Thus, increases in warm days in northern and central stations are consistent with a positive trend in Anticyclone over North Iberia/France; and negative trends in extreme precipitation in the East Cantabrian coast are consistent with a negative trend in the north-westerly flow. Furthermore, low-frequency temporal analyses reveal large (small) changes in extreme temperature (precipitation) days within the CTs. From the mid-1940s onwards, the extreme cold character of the northerly and north-easterly flows diminished, i.e. the frequency of cold nights within these CTs decreased from ~25 to ~15%, whereas from the 1920s to mid-1940s an opposite behaviour occurred (towards a higher frequency of cold nights). Throughout the 20th century, the frequency of warm days within the CTs has increased, especially for the south-westerly and westerly flows from the 1920s to 1950s and since the mid-1970s. Westerly flow was less frequent in the 1980s and 1990s but connected with a higher percentage of extreme precipitation days in West Iberia. This changing frequency of extremes within the CTs indicates that, apart from circulation types, other physical forcings have influenced the occurrence of extremes.

KEY WORDS: Winter circulation types · Iberian Peninsula · Daily extremes · Temperature · Precipitation · Within-type changes

1. INTRODUCTION

Climatic extremes are of particular interest for Mediterranean regions of high natural variability. Only slight shifts in precipitation and temperature extremes can lead to serious consequences for multiple sectors, such as agriculture, natural environment, infrastructure and human health. A comprehensive analysis is required to find the reasons for such variations, which are generally linked both to natural climate variability as well as to human-induced changes. Many recent studies have focussed on assessing changes in temperature and precipitation extremes on global (e.g. Alexander at al. 2006) or continental scales (over Europe, e.g. Moberg et al. 2006). For the Iberian Peninsula (IP; for further abbreviations see Table 1), Rodríguez-Puebla et al. (2010) found a significant increase (decrease) in the annual

*Email: soniafm@ual.es

Table 1. Abbreviations

Definitions of abbreviations and acronyms	
IP	Iberian Peninsula
SLP	Sea level pressure
SST	Sea surface temperature
SANDRA	Simulated ANnealing and Diversified Randomization clustering
CT	Circulation type
T_{max}	Daily maximum temperature
T_{min}	Daily minimum temperature
RR	Daily accumulated precipitation
TX90p	Warm days ($T_{max} > T_{max90th}$)
TN10p	Cold nights ($T_{min} < T_{min10th}$)
R90p	Extreme precipitation days ($RR > RR_{90th}$)
NAO	North Atlantic Oscillation
EA	East Atlantic pattern
EA/WR	East Atlantic/Western Russia pattern
SCA	Scandinavian pattern
M-K	Mann–Kendall test
SD	Standard deviation
PC(A)	Principal component (analysis)
CA	Cluster analysis

number of warm (cold) extremes during the second half of 20th century. Using the longest homogeneous series for Spain and Portugal, respectively, Brunet et al. (2007a) and Ramos et al. (2011) detected a sharp rise in extreme temperatures during the last third of the previous century, above all in summer and spring, while winter has contributed more to long-term warming. Changes in heavy precipitation, given the large inter-annual variability, are not clear and are more difficult to quantify. Gallego et al. (2011), assessing trends in the period 1903–2003 in 27 Iberian weather stations and for different rainfall categories, detected positive trends in wintertime days with precipitation >15 mm in the south- and north-west of Iberia. However, considering the second half of the 20th century, some negative trends are found in winter for heavy rainfall mainly in western parts of the IP, and positive trends in the south-east (Rodrigo & Trigo 2007, Rodrigo 2010, Gallego et al. 2011, Hidalgo-Muñoz et al. 2011).

Atmospheric circulation, especially in winter, is one main driver of regional changes in climate at mid-latitudes (Slonosky et al. 2001, Dunkeloh & Jacobeit 2003). The greenhouse effect seems to have exerted a clear influence on the increase of temperatures in Europe, and on the increasing (decreasing) trends in warm (cold) extremes detected since the beginning of 20th century (Moberg et al. 2006, Solomon et al. 2007). A key issue is whether circulation has also undergone changes — forced both by natural and, probably, human factors (the latter argued, e.g. by Corti et al. 1999) — and to what extent they explain fluctuations in mean climate as well as in the frequency and intensity of extremes. For example, Scaife et al. (2008), using climate models, showed the link between the increase in the North Atlantic Oscillation (NAO) index from the 1960s to the 1990s and the reduction in the occurrence of very low minimum temperatures in northern Europe.

Regarding large-scale circulation linked to regional climate anomalies in the IP, Rodríguez-Puebla et al. (2010) were able to associate fewer annual cold nights (1950-2006) to an increase in the EA teleconnection index, and more frequent warm days to a decrease in the SCA (Barnston & Livezey 1987). The negative phase of the EA/WR is related to intense precipitation in NW Iberia (Rodríguez-Puebla et al. 2001, Lorenzo et al. 2008). The NAO has a well-known influence on precipitation in Iberia (e.g. Rodrigo et al. 2001, Rodríguez-Puebla et al. 2001, Goodess & Jones 2002, Trigo et al. 2002, Gallego et al. 2005): its negative phase is linked to abundant precipitation in West, Central and Southern Iberia, mainly in winter. The extreme anomalies in precipitation during the winter of 2009–2010 (that caused severe damage in Southern Spain) occurred along with the most extreme negative NAO index ever measured (Vicente-Serrano et al. 2011). The NAO also exerts a clear influence on temperature in northern and central Europe, especially on minimum temperature variability and extremes (Trigo et al. 2002, Scaife et al. 2008, Guirguis et al. 2011). However, over southern Europe the effect of the NAO on temperature is complex and nonlinear, being extremely sensitive to the location of the SLP centres (Pozo-Vazquez et al. 2001, Castro-Díez et al. 2002).

There are different methods of analysing circulation changes: PCA methods provide large-scale modes of variability and teleconnection indices (Barnston & Livezey 1987); circulation indices built from the pressure difference between 2 stations are also widely used (Hurrell 1995, Slonosky et al. 2000, Trigo et al. 2002, Jones et al. 2003). Furthermore, a wide variety of classification-based methods (Philipp et al. 2010, Huth et al. 2008) can be applied. CTs are defined by classifying atmospheric dynamic fields (usually SLP or geopotential height), whereas weather types classifications also include additional meteorological variables, such as temperature or relative humidity (Bárdossy et al. 2002, Bermejo & Ancell 2009). Classification methods can be divided into subjective types, threshold-based methods and methods that produce derived types (Philipp et al. 2010). The subjective or 'manual' methods are based

on an expert knowledge of the synoptic climatology, such as the popular Lamb weather types catalogue (Lamb 1972) or that developed by Hess & Brezowsky (1952) for Central Europe. Examples of threshold-based methods include the objective versions of Lamb weather types using physical quantities (direction of flow, vorticity), e.g. adapted to Portugal by Trigo & DaCamara (2000), and used also by Lorenzo et al. (2008) and Ramos et al. (2010) in the NW of the IP. The methods that derive objective types are fully computer-based and comprise diverse techniques. Most of them use an optimization algorithm with the goal of achieving well separated and meaningful classes, such as neural network or cluster analysis (the most common being the non-hierarchical k-means CA). The classification is either done directly by means of a CA (Enke & Spekat 1997, Philipp et al. 2007, Küttel et al. 2010), or by a combination of multivariate techniques (PCA followed by a CA), such as Esteban et al. (2005, 2006), Romero et al. (1999), and Bermejo & Ancell (2009). A different approach is the use of climate regimes as a small number of quasi-stationary states of the atmosphere, obtained by classifying only days with persistent circulation (residence time of >5 or >10 d), shorter fluctuations being considered transitions between them. Although probably more suitable for analysing prolonged anomalies and extreme seasons (Cassou et al. 2005), some works have related these regimes with daily winter extremes for the North Atlantic (Yiou & Nogaj 2004) and Iberia (Ortiz Beviá et al. 2011).

Both teleconnection indices and circulation regimes are important for analysing large-scale atmospheric variability and persistence. However, centroid patterns derived from a CA as averages of many daily individual SLP fields should reflect better short-term phenomena, such as frontal temperature changes or heavy precipitation (Esteban et al. 2006, Philipp et al. 2007); hence, they may be more appropriate for analysing daily variables and extremes (Jacobeit 2010).

Circulation and weather-type classifications in the IP have been widely applied in precipitation studies (e.g. Romero et al. 1999, Trigo & DaCamara 2000, Goodess & Jones 2002, Lorenzo et al. 2008). Examples of other applications include fire hazards (e.g. Rasilla et al. 2010) or avalanches in the Pyrenees (Esteban et al. 2005). Changes in temperature within weather types in the second half of 20th century for Spain were studied by Bermejo & Ancell (2009). Also Jones & Lister (2009) showed changes in the response of temperature and precipitation to CTs for a set of European (including Iberian) stations, for 3 different periods in the 20th century, revealing an overall greater shift towards warming in winter. However, to the best of our knowledge, a detailed analysis of characteristic CTs and their influences on daily temperature and precipitation extremes over the whole IP, in the long-term, has not been attempted.

This paper follows the works of Philipp et al. (2007) and Jacobeit et al. (2009). The latter identified which CTs, derived in the former, are most conducive to extremes in Central Europe and analysed changes in those links. Here the objectives are (1) to explore the existence of trends in the frequency of extreme temperatures (warm days and cold nights) and precipitation (>90th percentile) in the IP over the longest period shared by all the series, i.e. 1950–2003; (2) to characterize winter circulation types over the IP from 1850–2003, assessing trends in the frequency also for 1950–2003; (3) to identify significant spatial relationships between CTs and local occurrences of extremes. Following this, we aim to search for concordant trends over 1950–2003 in both extremes frequency and CTs frequency; (4) to analyse temporal within-type variations (Beck et al. 2007), i.e. changes in the relationship between CTs and the mentioned extremes.

2. DATA

2.1. Station data

The database comprises daily series of minimum and maximum temperature (T_{min} and T_{max}, 29 Stations) and precipitation (RR, 44 Stations) across the IP until 2003 (Fig. 1, Table 2). These observations provide a reasonably good spatial coverage across Iberia. The stations are at various altitudes (from 7 to 1000 m above sea level, a.s.l.), with one station located in the Pyrenees mountains (1645 m a.s.l.). Table 2 also shows the source and length of the series. Of the 44 precipitation series, 20 cover the period 1911–2003, and the remainder start between 1913 and 1950. Of the 29 temperature series, 23 stations cover the period 1905–2003, and the remainder start at different dates between 1908 and 1947. Therefore, the longest period common to all station series is 1950–2003.

Most of the data come from the databases of Spanish Daily Adjusted Temperature and Precipitation Series (SDATS and SDAPS; Table 2). Their sources and homogeneity procedures are described in Brunet et al. (2006, 2007a,b). These databases have undergone quality control (QC) and homogenization by procedures similar to those described by the World

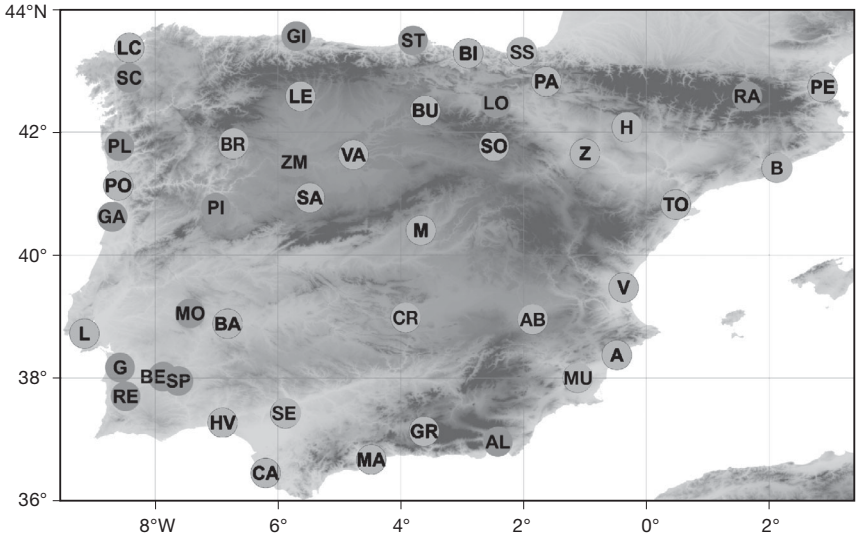

Fig. 1. Station database. Observatories with precipitation series (all 44 stations) and with T_{max} and T_{min} series (light gray, 29 stations). See Table 2 for acronyms

Meteorological Organization/World Climate Data Monitoring Programme Guidance on the development of daily adjusted temperature data sets (Brunet et al. 2008). Precipitation series from SDAPS have recently been used by Gallego et al. (2011). Homogenization procedures and QC of European Climate Analysis and Dataset (ECAD) series are described by Klein-Tank et al. (2002) and Klok & Klein Tank (2009). Homogenization of the Andorra-Ransol precipitation series is described by Esteban et al. (2009). Precipitation data from Portuguese Meteorological Institute (PMI) were provided by Instituto Dom Luiz (University of Lisbon) and were selected from the highest quality archives (Rodrigo & Trigo 2007, Rodrigo 2010). The Almeria precipitation series was supplied by the Spanish Agency of Meteorology (AEMET; www.aemet.es). The remaining precipitation series were provided by the University of Cantabria (Spain), sourced from ECAD and Regional Departments of AEMET, being really complete series (0 to 2% missing values) and free from spurious jumps or other inhomogeneities.

The completeness of all the temperature and precipitation series was tested, using the same criteria as those used by Moberg et al. (2006):

(1) First each series is checked to have sufficient daily values during the season-in-question to produce seasonal index values. A complete winter season is a 3 mo season (December–February) with <4 missing d.

(2) A complete series contains in each 20 yr block at least 10 complete winter seasons according to the above criterion. Blocks of 20 yr are defined as starting at the year given in Table 2; hence final blocks (ending in 2003) differ in length for each station and are checked for having more than of their seasons complete.

All T_{max} and T_{min} series fulfil the completeness criteria. Only 3 precipitation series, i.e. PA, SO and AB (see Fig. 1 and Table 2 for abbreviations), violate the abovementioned criteria for intermediate blocks. These RR series have 14, 11 and 17%, respectively, of missing values in the total period 1911–2003. Consequently, they are treated with caution and not considered for long-term average series in Section 4.4. All the other precipitation (temperature) series have <10% (<7%) of missing values over their complete periods.

Following Moberg et al. (2006), we use stricter criteria for the period shared by all stations (1950–2003), over which trends in the frequency of extremes are calculated. The first block, 1950–1969, and last block, 1984–2003, must contain at least 15 (out of 20) complete seasons. According to this criterion, T_{max}, T_{min} and RR series of AB, and RR series of PA are not complete and are rejected for the trend analysis.

Daily extreme indices are percentile-based, similar to indices defined by the Expert Team on Climate Change Detection, Monitoring and Indices (ETCCDMI, http://ccma.seos.uvic.ca/ETCCDMI, accessed January 2011), which allow for comparison between different regions. We analyse the following indices:

(1) Warm days (TX90p), as days on which T_{max} exceeds the station specific daily 90th percentile value of the reference period 1971–2000;

(2) Cold nights (TN10p), as days on which T_{min} falls below the station specific daily 10th percentile value of the reference period 1971–2000;

(3) Extreme precipitation days (R90p) as days on which the total precipitation amount is above the station seasonal specific 90th percentile of total daily precipitation on wet days (RR > 1 mm) in the 1971–2000 base period.

The 10th and 90th percentiles are taken to avoid potential inhomogeneities and jumps that are greater when a higher percentile (e.g. 95th, 98th) is used to define the threshold (Zhang et al. 2005), since very few extremes could be retained. The analysis is then focused on 'moderate' extremes. Nonetheless, while TN10p and TX90p have an average probability of 10%, the occurrence of R90p is less probable, since there are quite a lot dry days. TX90p and TN10p

Table 2. Description of station series of daily temperature (T_{min}, T_{max}) and precipitation (RR), latitude/longitude (DECLAT/DECLON, in decimal degrees), altitude (ALT, in m a.s.l.), beginning and source of the series (see Section 2.1). SDAT/SDAP: Spanish Daily Adjusted Temperature/Precipitation Series, PMI: Portuguese Meteorological Institute, ECAD: European Climate Analysis and Dataset, CENMA: Snow and Research Center of Andorra, AEMET: Spanish Agency for Meteorology

Station	Acronym	Declat	Declon	ALT (m a.s.l.)	Begin. (RR)	Begin. (T_{min}, T_{max})	Source
Cadiz	CA	36.5	−6.2	30	1911	1905	SDAP/SDAT
Madrid	M	40.4	−3.7	679	1911	1905	SDAP/SDAT
Barcelona	B	41.4	2.1	420	1911	1908	SDAP/SDAT
Huesca	H	42.1	−0.3	541	1911	1905	SDAP/SDAT
Murcia	MU	38.0	−1.1	57	1911	1905	SDAP/SDAT
Badajoz	BA	38.9	−6.8	185	1911	1905	SDAP/SDAT
Valencia	V	39.5	−0.4	11	1911	1905	SDAP/SDAT
Burgos	BU	42.4	−3.6	881	1911	1905	SDAP/SDAT
Salamanca	SA	40.9	−5.5	790	1911	1905	SDAP/SDAT
Alicante	A	38.4	−0.5	82	1911	1905	SDAP/SDAT
Soria	SO	41.8	−2.5	1083	1911	1905	SDAP/SDAT
Ciudad Real	CR	39.0	−3.9	627	1911	1905	SDAP/SDAT
Seville	SE	37.4	−5.9	31	1911	1905	SDAP/SDAT
Albacete	AB	39.0	−1.9	699	1911	1905	SDAP/SDAT
Granada	GR	37.1	−3.6	685	1911	1905	SDAP/SDAT
Valladolid	VA	41.6	−4.8	691	1911	1905	SDAP/SDAT
Huelva	HV	37.3	−6.9	19	1911	1905	SDAP/SDAT
Malaga	MA	36.7	−4.5	7	1911	1905	SDAP/SDAT
Zaragoza	Z	41.7	−1.0	245	1911	1905	SDAP/SDAT
Tortosa	TO	40.8	0.5	50	1911	1905	SDAP/SDAT
Coruna	LC	43.4	−8.4	67	1913	1905	SDAP/SDAT
Pamplona	PA	42.8	−1.6	452	1922	1922	SDAP/SDAT
Perpignan	PE	42.7	2.9	430	1924	1905	ECAD
San Sebastian	SS	43.3	−2.0	252	1928	1928	SDAP/SDAT
Ransol	RA	42.6	1.6	1645	1934		CENMA
Almeria	AL	37.0	−2.4	21	1934		AEMET
Lisboa	L	38.7	−9.2	77	1941	1905	ECAD
Porto	PO	41.1	−8.6	93	1941	1941	ECAD
Beja	BE	38.0	−7.9	246	1941		ECAD
Braganca	BR	41.8	−6.7	690	1945	1945	ECAD
Bilbao	BI	43.3	−2.9	35	1947	1947	AEMET
Pontelima	PL	41.8	−8.6	15	1948		ECAD
Leon	LE	42.6	−5.6	911	1948	1938	AEMET
Santiago	SC	42.9	−8.4	364	1948		AEMET
Zamora	ZM	41.5	−5.7	667	1948		AEMET
Gijon	GI	43.6	−5.7	30	1948		AEMET
Santander	ST	43.5	−3.8	59	1948		AEMET
Pinhel	PI	40.8	−7.0	600	1950		PMI
Serpa	SP	38.0	−7.6	190	1950		PMI
Gafanha	GA	40.6	−8.7	8	1950		PMI
Monfor	MO	39.1	−7.4	275	1950		PMI
Relíquias	RE	37.7	−8.5	270	1950		PMI
Grando	G	38.2	−8.6	94	1950		PMI
Logrono	LO	42.5	−2.5	352	1950		PMI

indices were also used, for example, by Alexander et al. (2006), Brunet et al. (2007a), and Ramos et al. (2011). To calculate temperature percentiles, we used an 11 d window centred on each calendar day. R90p days were studied by Kostopoulou & Jones (2005) in Greece in the framework of the project STARDEX (2005) and were termed heavy rainfall days.

2.2. Sea level pressure grids

In order to provide a long-term daily classification of the atmospheric circulation, reconstructions of mean SLP from the EMULATE project (European and North Atlantic daily to MULtidecadal climATE variability) are used. The development and quality features of the reconstructions are described in Ansell et

al. (2006). The spatial resolution of the dataset is 5° × 5°, and we make use of the complete available period 1850–2003. For the second half of 20th century, SLP EMULATE data explain ~90% of the variability of SLP from ERA-40 Reanalysis pressure data (ECMWF). The reason for such a good agreement is that pressure is a manageable variable to homogenize, and a small number of well-placed stations allow reliable reconstructions of the pressure fields, as argued by Slonosky et al. (2000). A domain between 30–50° N and 30° W–20° E was selected. Note that this sub-synoptic domain centred over the IP, to better account for large-scale circulation features, is larger than the D09 domain associated to the IP in the COST733 catalogue and used by Casado et al. (2010).

3. METHODS

3.1. Trends in extreme indices

The Mann-Kendall (M-K) non parametric method (Kendall 1938) was used to detect the presence of trends in the frequency indices (seasonal occurrence of TX90, TN10, and R90p days) at each station, over the complete shared period 1950–2003. The 5% significance level was used for all M-K tests.

In order to quantify the trends, a fit by least square linear regression was applied to the series of indices that show statistically significant trends for M-K. The significance of the linear model fitting was tested. Autocorrelation of the residuals was checked by means of the Durbin-Watson test: for large values of N, i.e. the number of observations, the null hypothesis of no autocorrelation can be accepted at the 95% confidence level when the Durbin-Watson statistic is between 1.40 and 2.60 (Wilks 1995).

3.2. Classification method

The method used to classify daily SLP fields is a non-hierarchical Simulated Annealing and Diversified Randomization clustering (SANDRA), described in detail in Philipp et al. (2007). The algorithm is based on conventional k-means clustering but differs in the ability to approximate the final solution (classification) to the global optimum. This improvement is achieved by simulated annealing: assignments of objects (daily circulation patterns) to clusters are allowed even if they increase the within-cluster variance and therefore corrupt the initial quality of the result. The occurrence of such assignments depends on a specific probability, which is slowly reduced during the classification procedure until convergence is reached. Casado et al. (2010) compared different classification methods for describing spatio-temporal variability of precipitation across Spain and found that SANDRA performs quite well for the 3 regions under consideration.

A non-hierarchical CA requires *a priori* specification of the number of clusters. This decision is reached here by the 'dominance criterion' (Jacobeit 1993, Philipp et al. 2007): the same SLP data-set is initially decomposed into independent classes (PCs) using t-mode Varimax-rotated PCA. To ensure that the extracted PCs are real manifestations of circulation variability and not artificial results of linear combinations, each of the extracted PC has to represent best the variability of at least one input variable (daily wintertime SLP-patterns) resulting in the maximum amount of the corresponding PC-loading. We also apply further restrictions: all the PCs must explain >1% of the variability and contain at least one case with a loading factor >0.5.

3.3. Trends and features of the CTs

An advantage of the SANDRA algorithm over conventional k-means CA is the achievement of more stable clusters; hence it increases confidence in the temporal frequency of the clusters (Philipp et al. 2007).

The M-K test is used to detect the existence of significant (p-value < 0.05) trends in the frequency of each circulation type for the whole period 1851–2003, and for the more recent period 1950–2003 (the period common to all stations series, in which trends in extreme indices are assessed). When significant trends occur, linear regression by least squares is conducted to quantify the trends. Trend-to-noise ratio test is used to estimate the significance of the linear trend. If the ratio is >1.96, an uninterrupted linear trend is significant at the 95% confidence level (Philipp et al. 2007). Additionally, normalized series of cumulative anomalies of the frequency have been analysed. They are assessed for each year as the difference between the frequency of the cluster and its mean long-term frequency (in 1850–2003); after that, cumulative series are obtained adding all the previous anomalies to the target anomaly. To normalize, the former series are divided by the standard deviation of the cumulative anomalies of the frequency.

The Spearman's rank correlation test is applied between seasonal CT frequencies and seasonal time

series of Northern Hemisphere (NH) teleconnection indices. These correlations help to interpret the derived CTs in terms of their large-scale circulation characteristics. The monthly indices series of the most meaningful modes for the Iberian climate (Rodríguez-Fonseca & Rodríguez-Puebla 2010, Ramos et al. 2010), i.e. NAO, EA, EA/WR, and SCA, are obtained from the Climate Prediction Center (CPC; www.cpc.ncep.noaa.gov/). Seasonal values are derived from averaging December, January, and February values for the available period 1950–2003.

3.4. Relating the CTs to the occurrence of extremes

The occurrence of temperature and precipitation extremes was analysed for each CT and each station. The mean efficiency of every CT to give rise to extremes at each location was measured by an index called index EF for the period 1950–2003, the longest period shared by all stations. This index (Jacobeit et al. 2009) is the quotient of the percentage of extreme days that occur in the CT (from total extreme days at the station) divided by the percentage of non-extreme days in the CT (from total non-extreme days at the station). Obviously, days with missing values are not included for the computation of the index. The index EF is assessed at 99% confidence level by means of Monte-Carlo resampling of 1000 series. That is, from all winter days in 1950–2003 (4814 d), 1000 different values of the index are obtained from 1000 random samples (all of them with 4814 d, with repetition). The 1000 index-values are then arranged in ascending order. The value in the position 10/1000 is taken as the index EF, thus having 1% of significance level. When this index EF exceeds the value of 1, the particular CT is considered as significantly conducive to extremes at the station in question, i.e. the CT is related to higher contribution to extreme days than to non-extreme days.

Relationships between CTs and surface meteorological variables are not always stable over time (Jacobeit et al. 2009, Küttel et al. 2010), but can vary on interannual and/or interdecadal time scales; Therefore, it is necessary to account for these variations by additional indices. As justified by Jacobeit et al. (2003) and Beck et al. (2007), the use of a 31 yr moving average is appropriate for studying these low-frequency within-type changes. We use two simple measures to study changes in the frequency of temperature and precipitation extremes within the CTs. Both are expressed as percentages and assessed for 31 yr windows. (1) The extreme potential of a given CT is defined as the proportion of all the days within that CT that are extreme. (2) We consider the overall contribution to extremes of a given CT as the proportion of all extreme days (irrespective of CT) that occur within that CT.

4. RESULTS

4.1. Trends in extreme indices (1950–2003)

Fig. 2 depicts the trends detected for the occurrence of extremes over the longest shared period 1950–2003. The orientation of the triangles represents the sign of the M-K statistic (see Appendix for the use of abbreviations). Black circles around them represent trends that are significant at the 5% level. A decrease (increase) is observed in the occurrence of cold nights (warm days) during the period, with significance at 12 (10) out of 28 stations. In general, trends in TN10p (Fig. 2a) are of higher magnitude than in TX90p (Fig. 2b), and both are of much higher magnitude than the few significant trends that occur in R90p (Fig. 2c). The magnitude of the linear trends is plotted on the maps (filled black colour) only when they reach the 5% significance level and the Durbin-Watson test indicates no autocorrelation in the residuals.

For TN10p, significant negative trends were found in the Mediterranean fringe (B, V, MU, A), southwest (SE, CA), Atlantic stations (L, LC), LE, SO, H and M. The magnitudes of the trends are between –1.0 and –2.9 d decade^{-1}. Most of the stations are located near the coast, which suggests the possible influence of the sea, e.g. because of the effect of increased sea surface temperatures (SSTs) on the trends. Additionally, an urban effect seems to be present in these trends as many of these stations (M, B, V, SE, L) are in large cities that have grown significantly since the 1950s. Nevertheless, the series were homogenized to minimize urban heat island effect (Brunet et al. 2007a), and we see that also negative trends appear in other smaller cities (SO, LE, H, A).

For TX90p, significant positive trends were found at 2 Mediterranean stations (V, B), and over North and Central Iberia (LC, M, CR, BI, BR, SA, BU, BA). The magnitudes of trends are between 1 and 2 d decade^{-1}. Therefore, over 1950–2003, smaller trends in TX90p than in TN10p are detected. This is in agreement with an overall greater increase observed in annual TN10p than TX90p over this period (Alexander at al. 2006, Rodriguez-Puebla et al. 2010).

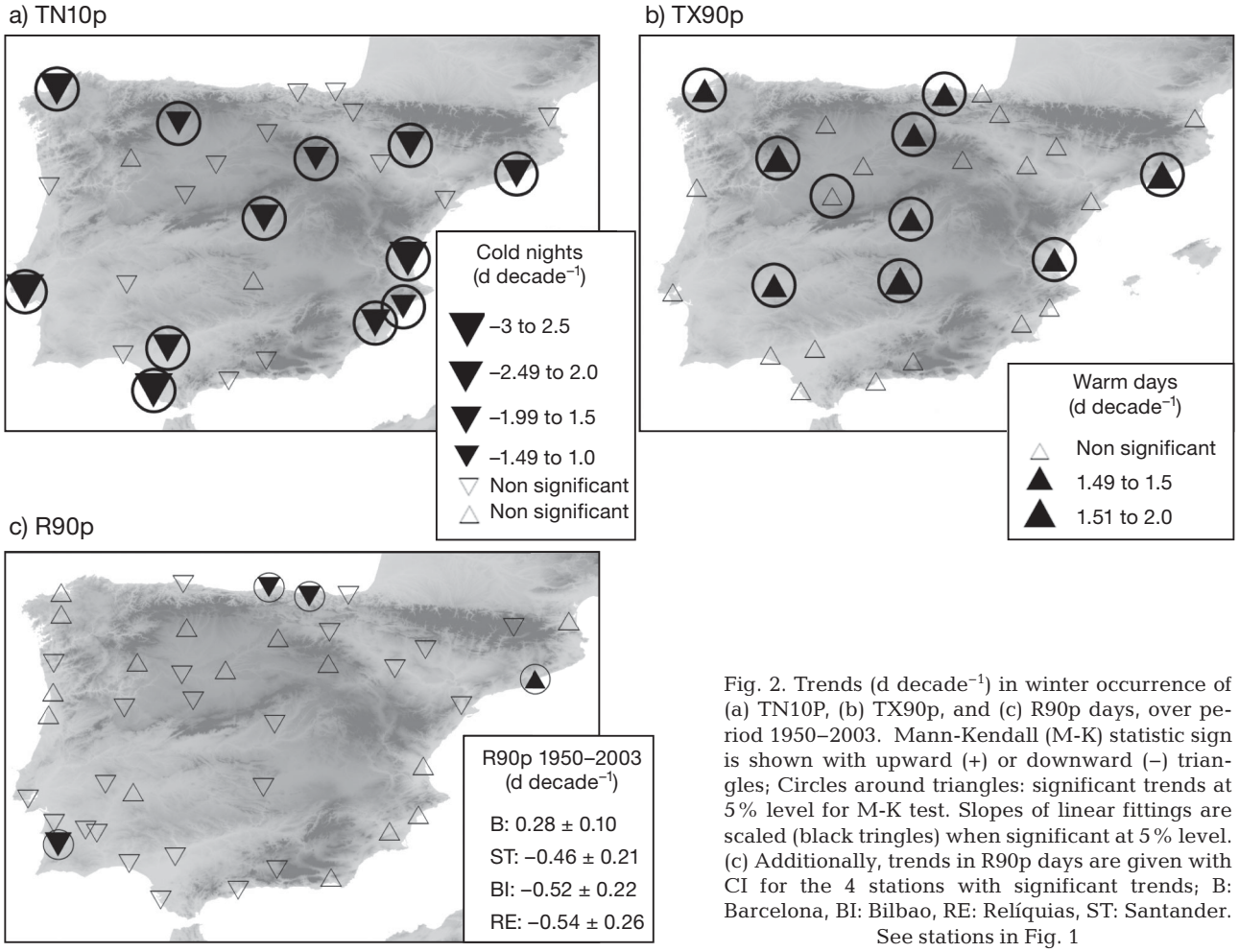

Fig. 2. Trends (d decade^{-1}) in winter occurrence of (a) TN10P, (b) TX90p, and (c) R90p days, over period 1950–2003. Mann-Kendall (M-K) statistic sign is shown with upward (+) or downward (–) triangles; Circles around triangles: significant trends at 5% level for M-K test. Slopes of linear fittings are scaled (black tringles) when significant at 5% level. (c) Additionally, trends in R90p days are given with CI for the 4 stations with significant trends; B: Barcelona, BI: Bilbao, RE: Relíquias, ST: Santander. See stations in Fig. 1

For R90p days, in general, positive (negative) trends appear in the Mediterranean fringe and at some stations in the northwest of the Iberian Peninsula (the remainder of the Peninsula). This regionalization seems to reflect, among other factors, the importance of the NAO pattern for intense rainfall over West and Central Iberia (Gallego et al. 2005), with predominance of positive phases in the 1980s and 1990s (Jones et al. 2003, Lorenzo et al. 2008). However, trends are significant only at 4 stations: negative trends at BI and ST (east Cantabrian coast) and RE (southwest), and positive trend at B (northeast Mediterranean station).

4.2. Description of the circulation types (1850–2003)

Fig. 3a presents the 7 CTs derived for the winter season: the cluster centroids represent the average of all daily SLP-patterns of each of the distinct clusters and are shown with the highest pressure values (in hPa) in red and the lowest in blue. Altogether, 13 897 d were classified, and the clusters are sorted according to the number of days belonging to each (first class = 2594 d, i.e. 18.6% of the days; second = 15.9%, etc.). Note that we sometimes refer to the CTs as 'clusters', since they are derived from a CA of SLP (Fig. 3). Fig. 3b displays the seasonal frequency of the distinct CTs in the period 1851–2003 (black bars) and normalized series of cumulative anomalies of the frequency (blue lines). Table 3 shows Spearman rho correlations (r) taking the available period 1950–2003 between the wintertime CT-frequencies and different meaningful teleconnection indices. Trends in the seasonal frequency of the CTs are presented in Table 4 (significant values in bold). The trend-to-noise ratio test shows that there is no CT that follows any uninterrupted linear trend (no values >1.96 in the long or the short period). Below, the 7 CTs are described separately.

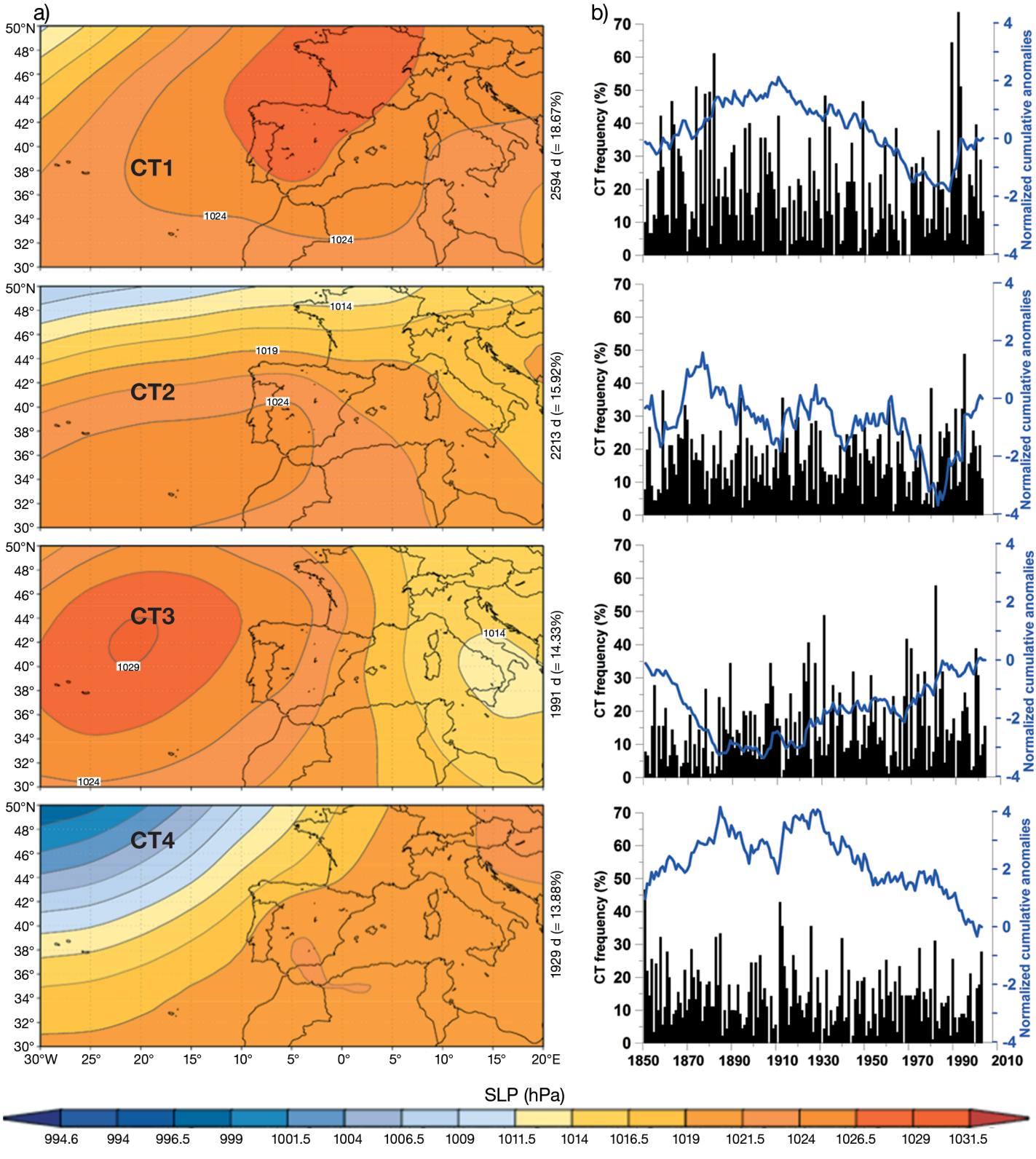

Fig. 3. (Continued on next page) Circulation types (CTs) 1–7 (a) centroid patterns of the SLP clusters and (b) seasonal frequencies (%) (bar charts, left axis) and their normalized cumulative anomalies (blue line, right axis)

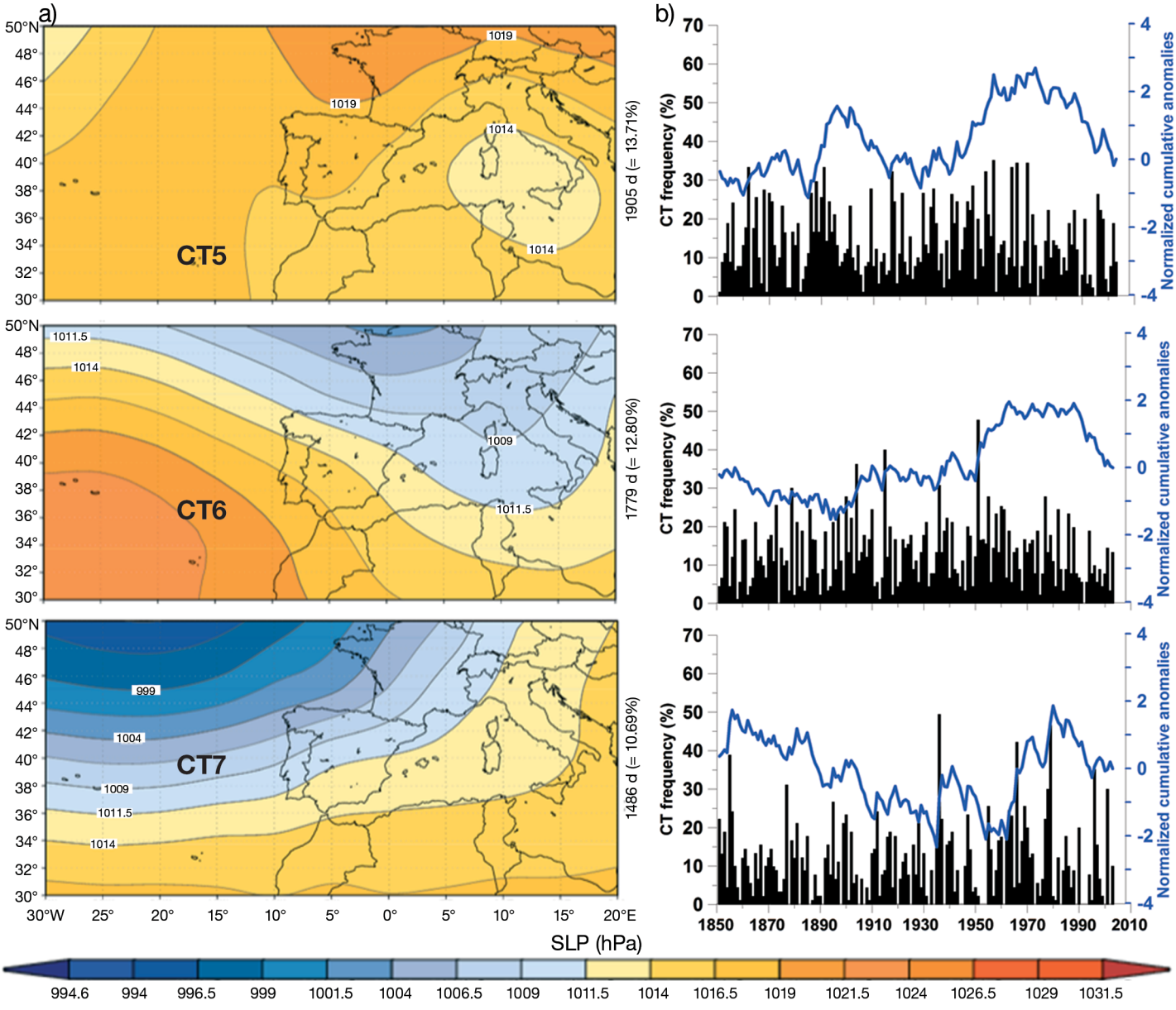

Fig. 3. (continued)

The CT1 centroid pattern (Fig. 3a, top panel) depicts a strong, north-eastward extended, subtropical high. CT1 decreases in frequency during most of the decades in the 20th century, with a rise in frequency from the 1980s onwards. There is a non-significant trend for the long period (1850–2003), but a significant positive trend in 1950–2003 according to M-K test (Table 4). It correlates positively with NAO (r = 0.47) and EA/WR (r = 0.59), and negatively with SCA index (r = –0.49). The highest correlation, with EA/WR, is in accordance with the high pressure over the North of Iberia/Western Europe. The correlation with SCA agrees with the decrease in this index since the mid-1980s (Lorenzo et al. 2008).

The CT2 pattern represents a situation with an eastward extended Azores high, prevailing north-westerly winds over Iberia and zonal flow further north in West Europe. It exhibits a positive NAO-correlation (r = 0.46). CT2 shows a low inter-annual variability but a high variability on multi-decadal time scales. The pattern is quite similar, although here with a smaller window, to the large-sale cluster 1 pattern of Philipp et al. (2007), also positively correlated with NAO and with similar fluctuations.

CT3 represents a meridional (northerly flow) pattern with a steep gradient between the Azores High and low over southern Italy. This pattern increased in frequency in the course of the previous century, with a significant positive trend according to the M-K test (Table 4). CT3 correlates positively with NAO (r = 0.5) and negatively with the EA pattern (r = −0.39).

CT4 shows the Icelandic low pressure centre displaced further east, with southwesterly flow over Northwest Iberia. The positive correlation with EA (r = 0.51) is coherent since low pressure is strong over the North Atlantic. It correlates positively with the SCA pattern (r = 0.35). CT4 decreases in frequency throughout the 20th century, with a significant negative trend (Table 4). CT4 is similar to cluster 6 in the classification of Philipp et al. (2007), which also shows a significant negative trend in 1851–2003 and decreasing frequency from the 1920s.

The CT5 centroid pattern presents a low pressure over the western Mediterranean/Italy, with weak pressure gradient except for a northeasterly flow over Spain. Its frequency shows positive anomalies from 1950–1970, decreasing after that, with a (non-significant) negative trend from 1851–2003. It correlates negatively with NAO (r = −0.59), which is meaningful since the relative low pressure over South Iberia and high pressure over northern France block the westerly flow towards Central Europe.

The CT6 pattern depicts low pressure over Northern France and Azores High displaced south in the North Atlantic, with northwesterly flow over Iberia. CT6 pattern has a negative EA/WR correlation (r = −0.45), which is supported by the low pressure over Northern France. It also correlates with the SCA index (r = 0.45). CT6 frequency increased in the decade from 1950 to 1960, decreasing in the 1990s (Fig. 3b). Furthermore, a significant negative trend is detected between 1950 and 2003 (Table 4), congruent with the abovementioned SCA correlation.

CT7 depicts prevailing westerly to southwesterly flow over Iberia resulting from the southward displaced and intensified low pressure centre (Icelandic low) in the North Atlantic; hence the high negative correlation (r = −0.72) with the NAO index. It exhibits high inter-annual variability and positive anomalies of frequency during 1960–1980.

4.3. Distributions of T_{max}, T_{min}, and RR for each CT

Box plots in Fig. 4 show distributions of daily T_{max}, T_{min} and RR for each of the CTs at selected representative stations, to explore discrimination among values for the distinct CTs.

Regarding T_{min} (Fig. 4a), the selected stations (CA and SA) have in common low values for CT3 and CT5, i.e. northerly and northeasterly flow patterns. In addition, the SA station shows low distributional values for CT1, probably because of cold east/northeasterly advection and clear sky conditions linked to the high pressure core. In both stations, distributional values of T_{min} are clearly the highest for CT7, which is reasonable because of the wet/warm advection from the Atlantic Ocean and cloudiness associated to the cyclones and storm tracks mainly over western Iberia. Also CT4 depicts west/southwesterly flow that brings wet and warm air from lower latitudes.

For T_{max} (Fig. 4b) the lowest distributional values are obtained for CT5, both for Alicante (A, southeast) and San Sebastian (SS, northern coast), probably due to cold continental advection as well as cloudiness linked to cyclone activity. For CT3 (North advection) T_{max} values are also low. The highest values of T_{max} are not so well discriminated among the CTs but the 'warmest' types for A (SS) are, in order, CT7, CT2 and CT4 (CT7, CT4 and CT2).

Focusing on winter precipitation distributions (Fig. 4c), for Seville, the wettest type is CT7, and the driest one is CT1. The CT7 pattern indicates a negative NAO situation characterised by a weak Azores High and southward shifted Atlantic storm tracks. This is a well-known pattern for producing positive precipitation anomalies in Iberia, mainly in the western parts. For Perpignan (PE) (Fig. 4c, right panel), CT5 clearly presents the highest RR values (90th percentile of daily RR for PE within CT5 is ~45 mm). The extended low pressure over southwest Italy (see Fig. 3a) must be understood as an average of diverse cyclonic centres over the area, being the most important in winter the cyclogenesis in the Gulf of Genoa-Lyon-Balearic and south of Italy (Trigo et al. 1999). The formation of Mediterranean cyclones may cause intense precipitation in the Mediterranean fringe especially near the cyclogenesis area. For PE, CT1 is the second wettest type, which is meaningful because of the prevailing easterly winds.

4.4. Relationships between CTs and moderate extremes

In this section the spatial relationships between CTs and extremes (TX90p, TN10p, and R90p, see Section 2.1) are quantified and discussed in terms of the index EF (obtained for the period 1950–2003) de-

Table 3. Significant Spearman rho correlations (associated CI at 5% significance level) between circulation type (CT) frequency and Northern Hemishpere teleconnection indices (Dec–Feb, 1950–2003). In case of CI including a zero value, correlation coefficients are not shown (dashes)

CT	NAO	EA	EA/WR	SCA
1	0.47 (0.26 to 0.75)	–	0.59 (0.42 to 0.83)	−0.49 (−0.72 to −0.30)
2	0.46 (0.23 to 0.73)	–	–	–
3	0.51 (0.34 to 0.74)	−0.39 (−0.66 to −0.19)	–	–
4	–	0.51 (0.33 to 0.77)	–	0.35 (0.11 to 0.63)
5	−0.59 (−0.84 to −0.44)	–	–	–
6	–	–	−0.45 (−0.75 to −0.22)	0.45 (0.26 to 0.69)
7	−0.72 (−0.90 to −0.62)	–	–	–

Table 4. Trends in frequency of circulation types (CTs) in 1851–2003 and 1950–2003. Mann–Kendall statistic Z(M-K) in **bold** are significant (p-value < 0.05). Linear trend: total magnitude in the period (days per 153 years and days per 54 years respectively). t:noise = quotient between linear trend and SD. No significant linear trends are detected (t:noise > 1.96)

CT	1851–2003				1950–2003			
	Z(M-K)	p	Trend	t:noise	Z(M-K)	p	Trend	t:noise
1	−0.56	0.574	−1.78	−0.14	**2.08**	**0.040**	13.91	1.09
2	0.47	0.635	1.13	0.14	0.51	0.612	3.40	0.40
3	**3.03**	**0.002**	7.16	0.73	0.21	0.834	1.18	0.12
4	**−2.07**	**0.038**	−4.76	−0.58	−0.03	0.976	0.40	0.06
5	−0.90	0.368	−1.51	−0.19	−1.69	0.096	−6.70	−0.84
6	−0.18	0.861	−0.44	−0.06	**−3.07**	**0.003**	−10.54	−1.48
7	−0.37	0.710	0.20	0.02	−0.64	0.533	−1.67	−0.17

scribed in Section 3. We interpolated the index EF from the 29 temperature and 44 precipitation stations using a simple algorithm with the inverse of the squared distance (Figs. 5a, 6a, 7a). Black lines delimit the influence of the type, i.e. stations with index EF >1 (significant at the 1% level). However, only values at the stations are strictly valid and taken into account in what follows.

In addition, the temporal variations in the extreme behaviour of the CTs are studied (see Figs. 5b, 6b, 7b). Within-type variations are shown averaging the series of stations affected by the CT, i.e. the longest period is 1905–2003 for temperature and 1911–2003 for precipitation extremes (see Table 2). Since 31 yr moving averages are used, the longest periods in these plots are, respectively, 1921–1988 and 1927–1988. The plotted lines and error bars in Figs. 5b, 6b, 7b (shadow) are the mean ± SD of the set of station series. The contribution of the CT to the total number of extremes (discontinuous black line, left axis) is plotted alongside the extreme potential of the CT (solid grey line, right axis).

4.4.1. Circulation types and cold nights (TN10p)

Concerning cold nights, 3 circulation types, CT1, CT3 and CT5, are found to be conducive to TN10p on the IP. Fig. 5a shows which Iberian stations are affected most by each of these CTs. The other 4 CTs have no influence (at 1% significance level) on the occurrence of cold nights at any station in the IP.

CT1 induces cold nights mainly in North and Central Iberia stations. The concomitant anticyclone core above northern/north-eastern Iberia (see Fig. 3a) causes clear-sky conditions that allow strong night-time radiative losses at surface levels. Furthermore, the advection of cold air masses from the northeast may lead to cooler air temperatures in northern and central parts of Spain.

CT3 is characterized by strong advection from the north, i.e. a southward displacement of Arctic air masses, due to the pressure gradient between a low in the Mediterranean Sea and the Azores High. This pattern is connected with cold nights over mainland Iberia, except for some northern and Ebro Valley stations (where the air masses still have maritime features). The cold character of the Arctic air masses may be enhanced by a cold katabatic effect.

CT5 represents advection of air masses from the northeast, from continental Europe, due to the low pressure over the Gulf of Genoa-West Italy and relative higher pressure over Central Europe. This flow is connected to cold and dry conditions, and represents the CT most conducive to cold nights over the whole IP, especially to the Northeast.

Regarding CT1 (averaging the LC, SA, BU, PE, A, BA, CR, VA, SO, Z and TO series; see Fig. 1), we ob-

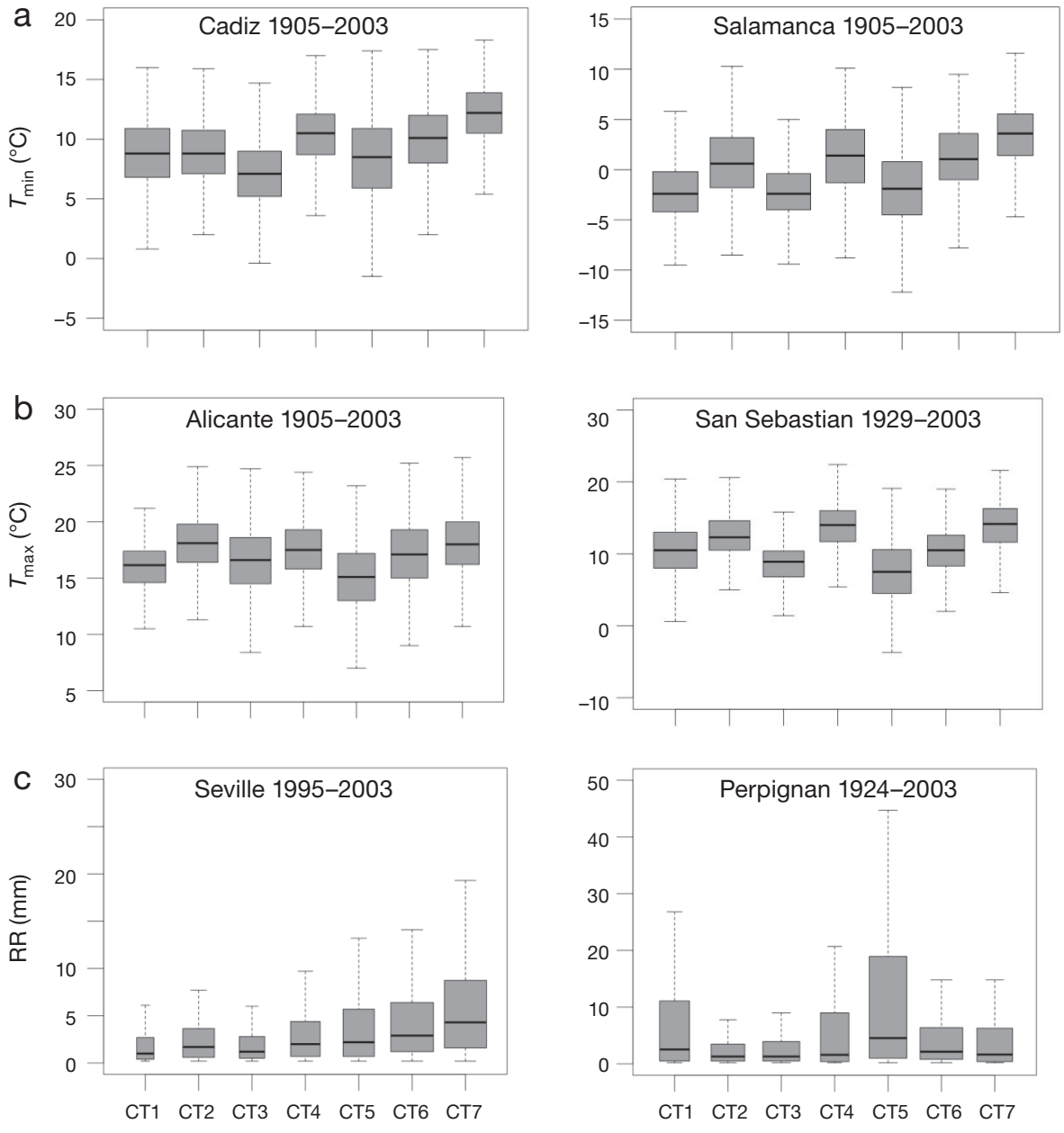

Fig. 4. Box-plots of daily (a) minimum (T_{min}) and (b) maximum (T_{max}) temperatures, and (c) precipitation (RR) from wet days (RR, days with RR ≥ 1 mm) composites for each of the circulation types (CT1–7), in 6 locations. Box-plots: median (central black line), 25th and 75th quantiles (limits of boxes), and 10th and 90th percentiles of distributions (top and lower extremes of plots)

serve an increase from the 1960s in its contribution to the total TN10p (Fig. 5b: dashed line in first panel; from 20 to 30%), which results in part from the positive trend in its occurrence in 1950 to 2003 (Table 4). However, the extreme cold potential of this type shows a slight decrease throughout the 20th century (grey line).

For the northerly type CT3 (averaging CA, SE, BA, L, SA, VA, M, CR, MU, A, V, B, H, HV, GR, MA and AB) a generalized decrease in the extreme cold potential from the 1950–60s onwards becomes visible, since the frequency of cold nights within the type drops from ~25 to 15%. From the 1920s to the 1950s, an opposite — but less pronounced — behaviour is

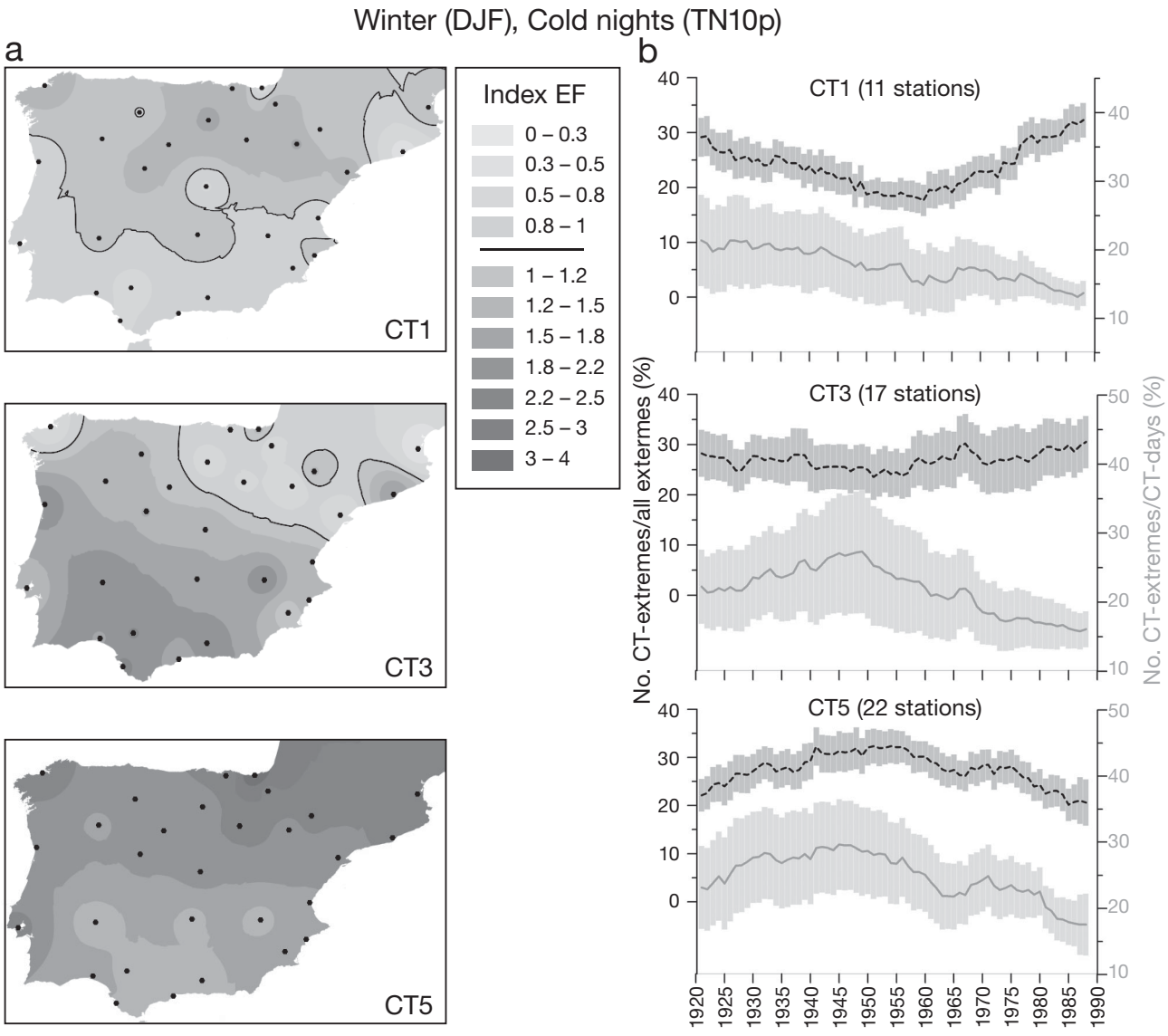

Fig. 5. (a) Index EF (see definition in Section 3.4) at 1% significance level, for circulation types (CTs) (see Fig. 3) conducive to cold nights (TN10p: $T_{min} < T_{min10th}$). Black line: index EF = 1 (stations with index EF >1 are considered affected by CTs). (b) Mean series (lines) ± SD (shadow) of extreme potential for cold nights (ratio of CT-extreme days to all CT-days) (grey, right axis) and contribution to total cold nights (ratio of CT-extreme days to all extreme days) (dashed black line, left axis), using a 31 yr moving average for a set of stations affected by the cluster. DJF: Dec–Feb

observed, i.e. an increase in its cold extreme potential. The contribution of the type to total TN10p days at the stations remains almost constant (~30%).

The contribution of CT5 (averaging 22 stations available in 1905 to 2003) to the total TN10p days falls from the 1950 to the 1960s, counteracted by the greater importance of CT1. This is partially because CT5 has been less frequent since the 1950s (Fig. 3b). Additionally, its cold extreme potential (Fig. 5b, continous line, right axis) increases from the 1920s to the mid-1940s, and decreases since then up to the mid 1960s and from the 1980s onwards.

4.4.2. Circulation types and warm days (TX90p)

Fig. 6a shows the 4 out of 7 circulation types most conducive to TX90p days in Iberia. Apart from these CTs, we found the influence of CT6 on warm days at Z and MA, and CT3 at LE, M and H to be significant (index EF > 1, at 1% significance level).

CT1, with an anticyclone in the North of the IP, gives rise to warm days at many stations of the Northern Plateau. There is also influence over the southwest (Seville), due to easterly winds (which are likely to be warmed by a Föhn effect from the Malaga Mountains).

This type gives rise to large daily thermal amplitude over many parts of the northern half of Iberia.

CT2 is related to warm days in the Mediterranean Fringe and Ebro Valley, due to an intensification of the Azores High (related to a positive NAO index) resulting in a west/northwesterly flow (from inland) over these areas.

CT4 is associated with warm days at the Cantabrian Coast because of flow from the South (inland). This centroid pattern represents the introduction of air masses from lower latitudes, leading to significant high maximum temperatures in many stations across the IP.

CT7. The zonal circulation (cyclonic westerly flow) is associated with warm days in the Mediterranean Fringe and parts of Central and Northern Iberia. This is due to the temperate and humid character of these maritime air masses, which, in turn, favour a Föhn effect in the lee of the mountain chains.

Fig. 6b shows the changes in the percentage of TX90p due to the mentioned clusters, using average percentage series (1905 to 2003). The first feature that stands out is the long-term increase in the warm-extreme potential of the types (grey continuous lines) through the previous century, particularly in the 1980s onwards, in contrast with the decrease in cold nights, which is more confined to the second half of the century.

Anticyclonic CT1 (averaging LC, SE, SO, BU, M) shows this progressive increase of its warm extreme potential, as well as an increase in its contribution to total extremes at the stations. The latter is mainly due to its trend in 1950 to 2003 (Table 4).

Within CT2 (averaging L, HV, MA, GR, MU, A, V, TO, Z, H, B, and PE), the extreme warm potential of the type increases mainly in the 1980s, which also makes its contribution to the total number of extremes higher in that decade.

CT4 (averaging L, LC, SE, GR, AB, BA, SA, VA, SO, and H) shows a rise in its extreme potential from the 1920s to the 1950s. Its average contribution to the total number of warm days dropped from the 1970s onwards, coincident with decreasing anomalies of its frequency (Fig. 3b).

A long-term increase in warm days within CT7 is observed (15 stations), even though in the last decades the frequency of this type has diminished (Fig. 3b: bottom panel). The increase in its warm extreme potential is more distinct from the 1970s onwards. However, its contribution to the total number of warm days falls from the 1960s and notably in the 1980s, when CT1 and CT2 were more frequent and contributed more.

4.4.3. Circulation types and extreme precipitation days

Fig. 7a depicts the CTs that are conducive (at 1% significance level) to R90p days at local stations. Apart from these types, CT4 is conducive to R90p days at Santiago (SC; to the northwest, not shown).

CT1 is significantly conducive to R90p days at V and MU. The large thermal contrast between the air (cold advection from east/northeast) and Mediterranean SST (warmer at these latitudes) can provide moisture and instability to low-level air masses. This, together with mesoscale factors (orographic or convective), may favour heavy rainfall. Doswell et al. (1998) studied one example of this kind of winter-intense rainfall event in southeast Iberia, which took place from 31st January to 6th February 1993. Some regions in the Mediterranean Fringe (mainly V, MU and Almeria provinces) recorded high daily precipitation. In our classification all these 7 d where classified as Type 1. The synoptic situation documented by Doswell et al. (1998) reflected high pressure over West-Central Europe and surface easterly winds reinforced by the presence of an Algerian low. Although such sub-synoptic scale systems are represented with difficulty in our classification (average 2594 d in this pattern), our method is able to identify the influence of this pattern in the southeast.

CT3 is conducive to R90p days at Bilbao [BI] and Pamplona [PA] stations. Cold and humid flow from the north/northwest (of arctic maritime origin) arrives at this coast often accompanied by strong winds (due to the steep pressure gradient). The formation of cold fronts may cause extreme precipitation, with high probability of snow. That was the case on 5–7 February 1983, each classified as CT3, with high records of precipitation (15 to 20 mm) at BI, PA and SS.

CT5 presents a western Mediterranean low and high pressure in Europe. On the southern limb of this anticyclone, cold and dry northeasterly flow over the Western Mediterranean gives rise to local cyclogenesis. Hence this type is prone to extreme precipitation days in the Mediterranean Fringe. PE is the station most influenced by this type, because it is located close to the influence of the 'Genoa low' system. The influence of the type over the southwest of the IP is explained by the relatively low pressure around the Gulf of Cadiz (formation of cyclones). Its negative correlation with NAO indicates the presence of a North-South dipole associated with intense precipitation over western and southern Iberia (Rodríguez-Puebla et al. 2001, Muñoz-Díaz & Rodrigo 2004).

In CT6, the pressure gradient indicates northwesterly circulation that allows wet air from the Atlantic

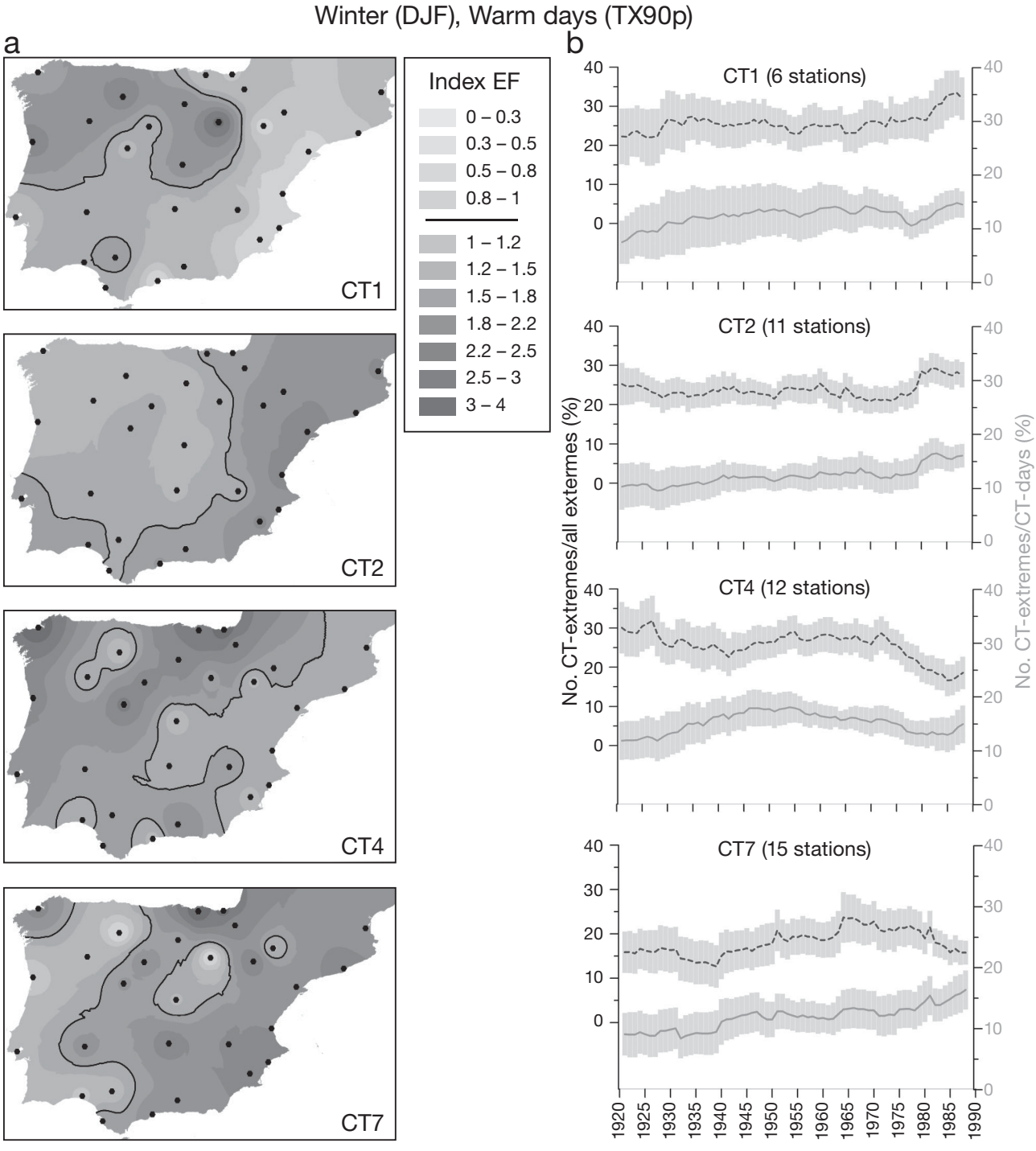

Fig. 6. As Fig. 5, but for occurrence of warm days (TX90p), for temperatures $T_{max} > T_{max90th}$

to arrive at northern and northwestern coasts. In addition, this CT has influence on Ransol (RA), coincident with the patterns conducive to heavy snowfall in the Pyrenees (Esteban et al. 2005). That is reasonable since the low pressure in the north of France may affect the Pyrenees, and the prevailing (cold and wet) north-westerly winds over the mountains generate abrupt ascent of the air, which favours intense precipitation, very likely as snow at those altitudes in wintertime.

In CT7, the shift to the south of the Icelandic low, and a steep meridional pressure gradient, leads to rel-

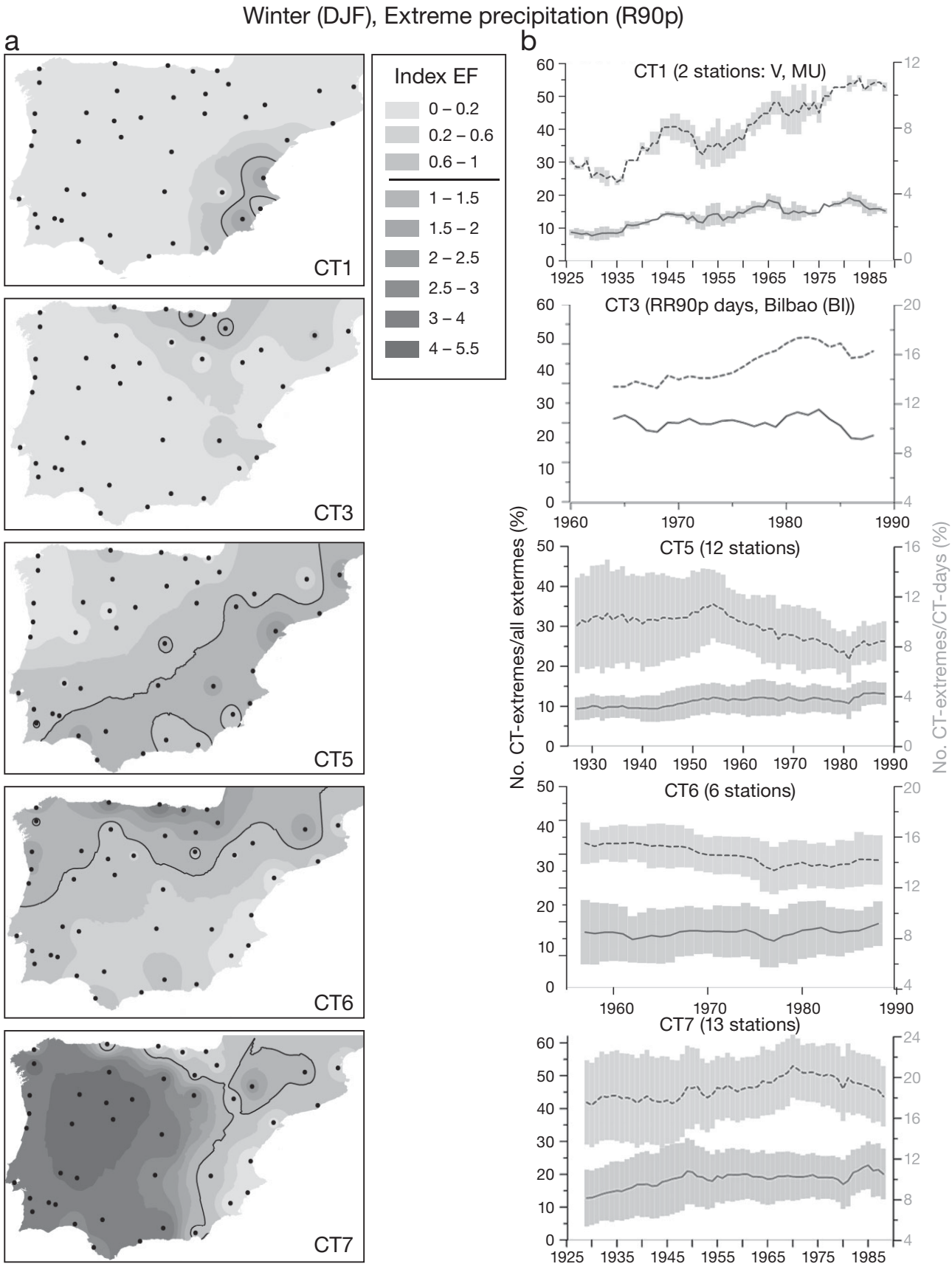

Fig. 7. As Fig. 5, but for extreme precipitation days (R90p): RR > RR_{90th}

atively strong westerly winds. These introduce wet and warm air to the Peninsula, conducive to moderate extreme precipitation over mid-West Iberia (except Mediterranean, Ebro Valley and Northern Coast stations). Many previous studies (e.g. Rodríguez-Puebla et al. 2001, Muñoz-Díaz & Rodrigo 2004, Gallego et al. 2005) have shown a link between NAO negative phase and precipitation in winter in West, Central and South Iberia. In Fig. 7a we also see the influence on heavy precipitation at H (541 m) and RA (1645 m) in the Pyrenees. This is in agreement with Vicente-Serrano et al. (2009), who found a negative correlation between daily NAO index and intense precipitation at high altitude stations in northeastern Iberia.

For precipitation extremes, variations in the extreme potential of the CTs (Fig. 7b) are lower than for temperature extremes, i.e. the relationship is more stable.

For CT1 conditions (easterlies), a slight increase in the wet extreme potential of the CT (V and MU stations) is observed. At the same time, and partially linked to significant increasing frequency of CT1, the contribution of this circulation to the total R90p days in the stations undergoes a stepped rise in 1940 to 1990 (from 25 to 50%).

CT3 variations in relation to R90p days (at BI) indicate a decline in the wet extreme potential of the type in the 1980s to 1990s. This explains the reduced contribution of the type to total R90p days, and, at least in part, the negative trend in R90p days detected at BI (Fig. 2c).

The wet extreme potential of CT5 (averaging HV, CA, SE, MA, CR, M, A, V, TO, B, Z and PE) shows small increases from the 1940s to mid-1950s and in the 1980s. The decrease in its contribution to total R90p days since the mid-1950s is therefore mostly due to its reduced frequency (Fig. 3b).

The CT6 wet extreme potential (averaging LC, SS, BU, SO and RA) is almost stable (~8%) throughout the second half of the 20th century, with a slight increase in the most recent decade (1978 to 1988). Its contribution to total R90p days at the abovementioned stations is ~35%, with a progressive decrease over the period (30% in recent decades), which is due to its decreasing frequency (Table 4).

The CT7 wet extreme potential (averaging MA, GR, CA, SE, HV, CR, BA, M, SA, VA, LC, BU and H) underwent increases in 1930–1950 and 1980–1988. The average contribution of this type to total R90p days shows a progressive increase over 1930–1970 (from 40 to 50%) and a slight decrease since the 1970s (from 50 to 40%); the latter in due to decreasing anomalies in its frequency (Fig. 3b).

5. DISCUSSION

The trends detected here over 1950 to 2003 (Fig. 2a–b) agree with previously observed variability and trends of extreme temperatures (Brunet et al. 2007a, Fernández-Montes & Rodrigo 2011, Ramos et al. 2011) in the Iberian Peninsula in winter. The few significant trends in extreme precipitation days (R90p, Fig. 2c) are also consistent with previous studies (Goodess & Jones 2002, Rodrigo 2010, Gallego et al. 2011, Hidalgo-Muñoz et al. 2011).

The study provides information regarding spatial and temporal links between circulation and winter extremes in Iberia. Better spatial discrimination is obtained for cold nights (only 3 cold types) and extreme precipitation (clear regionalization) than for warm days (4 extreme warm types and not as clear regionalization). Therefore, day-time warm conditions seem largely influenced by other variables and/or local factors. Indeed discrimination in T_{max} distributions (Fig. 4b) are not as great as T_{min} (Fig. 4a), and both are worse than the differentiation for RR distributions (Fig. 4c). Results indicate a decline in CT7 and CT4 (Fig. 3b, Table 4), which are related to the highest T_{min} (see Fig. 4a), contrary to the observed tendency towards warmer night time conditions (Brunet et al. 2007a,b, Ramos et al. 2011). The abovementioned studies also found a remarkable increase in average T_{max}, which might be related to increased occurrence of CT2 since the 1980s (see Figs. 4b & 3b). A recent rise in both T_{max} and T_{min} in the IP could also be partially explained by a decrease in the frequency of CT5 (Figs. 3b, 4a,b) from the 1970s onwards. It is worth noticing that in 2 of the coldest winters in the IP, i.e. 1891 and 1956, CT5 manifested a high frequency. However, CT3 has an overall positive trend (see Table 4) that would have led to enhanced occurrence of low T_{min} (Fig. 4a & 5a) during the whole 20th century. To some extent (according to Fig. 4c: left panel and Fig. 7a: bottom panel) we could attribute a recent drop in winter intense precipitation over the Southwest (found by Gallego et al. 2011, and here in Fig. 2c) to the changes in the frequency of CT1 (positive trend in 1950 to 2003, towards drier conditions) and CT7 (less frequent).

The use of long-term datasets potentially grants a basis for the development of synoptic-based downscaling techniques. Nevertheless, our study indicates that a non-stable relationship exists between CTs and extremes, i.e. other factors apart from circulation types are required to characterize temperature (precipitation) extremes, since large (small) low-frequency temporal variations are found (Figs. 5b, 6b, 7b). As in

other studies of Europe (Osborn & Jones 2000, Jacobeit et al. 2009, Jones & Lister 2009, Küttel et al. 2010), a 'warming within the circulation types' is found here, which is more evident for T_{min} indices and from the middle of the 20th century onwards (Fig. 5b). We will detail in the following which changes in the frequency of extremes may be linked to changes in the frequency of the CTs and which variations have occurred within the CTs, discussing possible physical mechanisms responsible for these variations.

Regarding the cold CTs, CT3 (which indicates advection from the North) shows a generalized decrease in its cold extreme potential from the 1950–60s onwards (Fig. 5b: middle panel). This implies a warming of the air that comes from the eastern North Atlantic Ocean to the northern coast of Spain, being insufficiently counteracted by the cold wintertime continent surface. These results are consistent with a rise in the SST of the Biscay Gulf from the 1970s to the present (De Castro et al. 2009). A remarkable decrease in cold nights during 1950–2003 has been detected in the Mediterranean area, similar to that found by Brunet et al. (2007a) for seasonal regional series, and, on an annual scale, by Rodríguez-Puebla et al. (2010). According to our results, fewer cold nights are due to both a lower frequency of CT5 and to a decreasing cold extreme potential of this type and of CT3. The decrease in cold nights within CT5, CT3 and CT1 is congruent with the results of Bermejo & Ancell (2009), which showed a generalized increase in T_{min} within a set of 100 weather types in Spain for 1980–2002 compared to 1957–1979. Anticyclone conditions represented by CT1 induce cold nights over northern Iberia, its contribution to TN10p increasing from 1960s onwards (see Fig. 5b: upper panel, where it accounts for >30%). Correlations with teleconnection indices indicate both a positive (CT1 and CT3) and negative (CT5) association with the NAO index, in agreement with the study of Castro-Díez et al. (2002). The negative (weak) correlation of CT3 with EA index supports the association found by Rodríguez-Puebla et al. (2010) between cold nights and the EA pattern.

Considering the warmest CTs (Figs. 3a, 6a), CT1, high pressure conditions over northern Iberia, favours warm days over the northern plateau and the southwest. CT1 exhibits a negative (positive) correlation with the SCA (EA/WR and NAO). The positive trend in the frequency of CT1 from 1950 to 2003, therefore, implies in general warmer conditions over the IP. Over this period, increasing trends are detected in TX90p days in all the stations affected by CT1 (Fig. 2b, significant trends at LC, BR, BU and M). These results are again consistent with Rodríguez-Puebla et al. (2010) who related the increases in TX90p days (annual) to a decrease in the SCA index. CT2 correlates positively with the NAO index and is conducive to warm days over the Mediterranean coast and Ebro valley. Moreover, both CT1 and CT2 show positive anomalies in frequency since the 1980s, which may have contributed to increases in warm days over that time period to the north- and south-west, respectively, of the IP. Besides CT1 and CT2, moderate warm days in winter are favoured (for a larger number of stations) by zonal circulation, i.e. flow from the West (CT7, correlated with NAO-) and Southwest (CT4, correlated with EA+). The positive trend in warm days at V, B, CR, CA, BA, SA and LC from 1950 to 2006 (Fig. 2b) are, to a large degree, linked to an increase in the warm extreme potential of the westerly flow (Fig. 6b: bottom panel). CT7 has increased its warm extreme potential, in particular in 1920–1950 and from the mid-1970s onwards. Since westerly flow transports heat from the Atlantic, this may be attributable, among other factors, to an underlying warming of Atlantic SSTs in those periods (Solomon et al. 2007, Ting et al. 2009). Congruent with a smaller recent increase in Mediterranean SSTs during winter (Nykjaer 2009), changes in the warm and cold extreme potentials of easterly flow (i.e. CT1) are less pronounced. Among other recent studies, Cattiaux et al. (2010) have showed that, added to North Atlantic atmospheric circulation, the consideration of SSTs helps to reconstruct recent European extreme temperatures (2003 to 2007), especially in autumn and winter. In addition, the increase in sunshine duration over the IP, albeit less pronounced in winter than spring, from the 1980s onwards (Sánchez-Lorenzo et al. 2007) has likely influenced the occurrence of extreme maximum temperatures.

Different CTs are conducive to R90p days for different regions. To the southeast, R90p days are linked to easterly flow associated to high pressure over North Iberia/France (CT1). CT1 increases in frequency during 1950–2003 (Table 4). Goodess & Jones (2002) also found a positive trend during 1957–1998 in the frequency of easterly flow, as did Esteban et al. (2006) during 1960–2001. Hidalgo-Muñoz et al. (2011) reported an increase in the frequency of the main synoptic pattern related to very heavy precipitation for the southeast. In addition, CT1 has slightly increased in wet extreme potential (Fig. 7b: upper row). Northerly flow (CT3, positive NAO-correlated) is conducive to R90p days at BI and PA. The wet extreme potential of CT3 diminished in the mid-1980s

(Fig. 7b: third row), which must in part be responsible for the negative trend detected at BI and ST (Fig. 2c). Additionally, northwesterly flow (CT6) is conducive to R90p days in the north (including BI and ST) and northwest of Iberia. The negative trend over 1950 to 2003 in CT6 would lead to less extreme precipitation days to the northern and northwestern coasts, as well as at Pyrenees stations (Fig. 7a: 4th row). Decreasing trends in R90p days are observed at the Pyrenees and Cantabrian coast stations (Fig. 2c). CT5 is conducive to R90p days in East and South Iberia. A lower occurrence (but non-significant trend) of CT5 in the second half of the 20th century could explain the (non-significant) negative trends in R90p days over Southwest and Central Iberia. The contribution of CT5 to the total number of R90p (affected stations) dropped from 30 to 20%, counteracted by higher contributions of CT7 in the southwest and CT1 in the southeast (see Fig. 7b). The type most conducive to R90p days at all stations located in West and Central Iberia is CT7. Only stations further east in the Mediterranean Fringe and Cantabrian coast are not affected by this CT. Its correlation with the negative phase of NAO is strong (rho = −0.72). Even clearer for CT7 than CT5 (that also exhibits NAO correlation, rho = −0.59), R90p days linked to CT7 (Fig. 7b: grey line, bottom panel) have slightly increased, especially from 1930 to 1950 and in the 1980s. This behaviour could partially explain the positive trends in intense winter precipitation days in southern and northwestern stations of Iberia during 1903–2003 detected by Gallego et al. (2011). Some previous studies have similarly shown a strengthening of the NAO–precipitation relationship in Europe in recent decades (Vicente-Serrano & López-Moreno 2008, Vicente-Serrano et al. 2011). This could be due to changes in the location and intensity of NAO action centres (i.e. the Icelandic Low and the Azores High) (Ulbrich & Christoph 1999, Ramos et al. 2010), which have shifted eastward in the most recent decades of our study (Jung et al. 2003). However, apart from anomalies in the surface circulation, anomalies such as those in the mid to high tropospheric flows (jet stream displacement) have proved to be crucial to explain some exceptional precipitation events (Vicente-Serrano et al. 2011). In this sense, more synoptic detail, than that given by this CT classification, would presumably help, and is clearly required for modelling high frequency changes and downscaling extremes, such as methods based on analogues (Brands et al. 2010). Here, by contrast, we have focused on recognizing important low-frequency changes: thus, for example, the periods of increasing wet extreme potential of CT7 (Fig. 7b: bottom panel) are almost coincident with the periods of increasing warm extreme potential (Fig. 6b: bottom panel). This is physically plausible, since warmer air is capable of holding more water content before saturation; therefore it can lead to greater volume of precipitation.

6. SUMMARY AND CONCLUSIONS

For the Iberian Peninsula, 7 circulation types (CTs) were derived from a cluster analysis of SLP (winter days in 1850 to 2003). The derived CTs have, unsurprisingly, a meaningful relationship with the occurrence of daily extreme events in distinct parts of the IP, with a better regionalization and discrimination for precipitation than temperature extremes. They also show meaningful correlations with NH teleconnection indices. The CTs show high interannual and interdecadal variability, without significant linear trends in frequency. Nevertheless, over the total period 1851–2003, northerly (southwesterly) flow has a positive (negative) trend according to M-K tests; in addition during 1950–2003, the lower frequency of the northwesterly flow was accompanied by more frequent easterly flow.

Regarding changes in extremes, from 1950 to 2003 (the longest period shared by all stations) we have found, consistent with other authors, significant negative (positive) trends in the frequency of cold nights (warm days). Trends in warm days are lower (~1.5 d decade^{-1}) than in cold nights(~−2 d decade^{-1}). Some of the trends may be linked to changes in the frequency of the CTs: advection from the northeast was less frequent in recent decades, in concordance with the decrease in cold nights observed in Mediterranean fringe, southwest and Atlantic sites. Moderate warm days in winter are favoured by circulation flow from the west and southwest. Also high pressure conditions over northern Iberia induce warm days over the northwest plateau and southwest. The positive trend in the frequency of this CT during 1950–2003 may explain the increase in warm days detected at some stations. Few trends exist in the frequency of extreme precipitation days (R90p days), which in general are positive in the east and negative in western and northern Iberia. The westerly flow circulation (highly negative NAO correlated) is the most conducive type to R90p days in west, central and south Iberia, as well as at high altitudes further to the northeast. Northwesterly (easterly) flow type has undergone a significant negative (positive) trend

over 1950 to 2003, which could partially explain the significant negative (non-significant positive) trend in R90p at east Cantabrian coast (Mediterranean Fringe) over this period.

In addition to relating the CTs with extremes in a time independent way, we went on to analyse temporal variations in the contribution and in the extreme potential of the CTs. That characterisation allowed us to make sense of the data and identify other important low-frequency effects during 1921–1988.

Variations in the frequency of temperature extremes within the CTs reveal that cold (warm) CTs have become less (more) conducive to extreme cold (warm) conditions: northerly and northeasterly advection patterns increased their cold extreme potential from the 1920s to 1950s, with a sharp decrease (warming) since then. Thus, the CT that contributed the most to cold nights progressively from the 1960s onwards is the anticyclone over North Iberia/West France. A rise in warm days at stations in the Mediterranean, the north and the southwest is connected with an increased warm extreme potential of westerly flow, especially marked in the 1980s. These changes may be attributable, among other factors, to changes in Atlantic SST. Regarding their wet extreme potential the CTs have undergone smaller variations. R90p days in western Iberia within westerly flow have been slightly more frequent from 1930 to 1950, and in the 1980s. Similarly, in Mediterranean and southern Iberia, R90p days were also more frequent in the 1980s within easterly and northeasterly CTs. In contrast, over the east Cantabrian coast, R90p days decreased in the 1980s under conditions of northerly flow.

This study therefore frames extreme events within characteristic CTs that show changes in frequency and extreme-producing potential over time. The IP is affected by polar and subtropical air masses and is influenced by both the Atlantic Ocean and the Mediterranean Sea. Thus, besides surface atmospheric circulation, variations in additional parameters (even if some of them are somehow related to SLP), such as SSTs, mid-troposphere circulation, air and soil moisture, solar radiation, greenhouse gases and aerosol concentrations etc., influence regional climate and its extreme behaviour. It is natural that some trends in daily extremes correspond to changes in the frequency of various atmospheric CTs, but low-frequency changes within the same CTs are notable, especially for temperature extremes. These instabilities should be considered before projecting future changes. The contribution to the occurrence of extremes of atmospheric dynamics together with other physical forcings (such as SSTs) needs to be studied in more depth and quantified in future research.

Acknowledgements. S.F.M. and F.S.R. were supported by the Spanish Ministry of Science and Innovation, project CGL2007-65546-C03-01. S.S. and E.H. were supported by the German Research Foundation, project KLIWEX-MED. The authors thank E. Aguilar from the Climate Research Group of the University of Rovira I Virgily (Tarragona, Spain) for providing SDATS and SDAPS data series. In addition, our most sincere thanks to R. M. Trigo (University of Lisbon, Portugal), D. Rasilla (University of Cantabria, Spain) and P. Esteban (CENMA, Andorra) for providing precipitation series. We also express our gratitude to COST733 project 'Harmonisation and applications of weather type classifications for European Regions' and A. Philipp (University of Augsburg, Germany) for providing the COST733 classification software. Finally, we thank the 3 anonymous reviewers for their constructive comments and suggestions which improved the manuscript.

LITERATURE CITED

Alexander LV, Zhang X, Peterson TC, Caesar J and others (2006) Global observed changes in daily climate extremes of temperature and precipitation. J Geophys Res 111:D05109. doi:10.1029/2005JD006290

Ansell T, Jones PD, Allan RJ, Lister D and others (2006) Daily mean sea level pressure reconstructions for the European–North Atlantic region for the period 1850–2003. J Clim 19:2717–2742

Bárdossy A, Stehlík J, Hans-Joachim C (2002) Automated objective classification of daily circulation patterns for precipitation and temperature downscaling based on optimized fuzzy rules. Clim Res 23:11–22

Barnston AG, Livezey RE (1987) Classification, seasonality and persistence of low frequency atmospheric circulation patterns. Mon Weather Rev 115:1083–1126

Beck C, Jacobeit J, Jones PD (2007) Frequency and within-type variations of large scale circulation types and their effects on low-frequency climate variability in Central Europe since 1780. Int J Climatol 27:473–491

Bermejo M, Ancell R (2009) Observed changes in extreme temperatures over Spain during 1957-2002 using weather types. Revista de Climatología 9: 45-61

Brunet M, Saladié O, Jones P, Sigró J and others (2006) The development of a new dataset of Spanish daily adjusted temperature series (SDATS) (1850–2003). Int J Climatol 26:1777–1802

Brunet M, Jones PD, Sigró J, Saladié O and others (2007a) Temporal and spatial temperature variability and change over Spain during 1850–2005. J Geophys Res 112: D12117. doi:10.1029/2006JD008249

Brunet M, Sigró J, Jones PD, Saladié O and others (2007b) Long term changes in extreme temperatures and precipitation in Spain. Contrib Sci 3:331–342

Brunet M, Saladié O, Jones PD, Sigró J and others (2008) A case study/guidance on the development of long term daily adjusted temperature datasets. WCDMP-66/WMO-TD-1425, WMO, Geneva

Casado MJ, Pastor MA, Doblas-Reyes FJ (2010) Links be-

tween circulation types and precipitation over Spain. Phys Chem Earth 35:437–447

Cassou C, Terray L, Phillips AS (2005) Tropical Atlantic influence on European heat waves. J Clim 18:2805–2811

Castro-Diez Y, Pozo-Vazquez D, Rodrigo FS, Esteban-Parra MJ (2002) NAO and winter temperature variability in southern Europe. Geophys Res Lett 29(8)

Cattiaux J, Vautard R, Yiou P (2010) North-Atlantic SST amplified recent wintertime European land temperature extremes and trends. Clim Dyn 36:2113–2128

Corti S, Molteni F, Palmer T (1999) Signature of recent climate change in frequencies of natural atmospheric circulation regimes. Nature 398:799–802

deCastro M, Gómez-Gesteira M, Alvarez I, Gómez-Gesteira JL (2009) Present warming within the context of cooling–warming cycles observed since 1854 in the Bay of Biscay. Cont Shelf Res 29:1053–1059

Doswell CA III, Ramis C, Romero R, Alonso S (1998) A diagnostic study of three heavy precipitation episodes in the western Mediterranean region. Weather Forecast 13: 102–124

Dunkeloh A, Jacobeit J (2003) Circulation dynamics of Mediterranean precipitation variability 1948–1998. Int J Climatol 23:1843–1866

Enke W, Spekat A (1997) Downscaling climate model outputs into local and regional weather elements by classification and regression. Clim Res 8:195–207

Esteban P, Jones PD, Martín-Vide J, Mases M (2005) Atmospheric circulation patterns related to heavy snowfall days in Andorra, Pyrenees. Int J Climatol 20:1599–1618

Esteban P, Martin-Víde J, Mases M (2006) Daily atmospheric circulation catalogue for Western Europe using multivariate techniques. Int J Climatol 26:1501–1515

Esteban P, Prohom MJ, Aguilar E, Mestre O (2009) Evolució recent de la temperatura i de la precipitació a Andorra (1934–2008): resultats anuals i estacionals. Centre d'Estudis de la Neu i de la Muntanya d'Andorra de l'Institut d'Estudis Andorrans (CENMA), Andorra

Fernández-Montes S, Rodrigo FS (2011) Trends in seasonal indices of daily temperature extremes in the Iberian Peninsula, 1929–2005. Int J Climatol 31 doi:10.1002/joc.3399

Gallego MC, García JA, Vaquero JM (2005) The NAO signal in daily rainfall series over the Iberian Peninsula. Clim Res 29:103–109

Gallego MC, Trigo RM, Vaquero JM, Brunet M, García JA, Sigró J, Valente MA (2011) Trends in frequency indices of daily precipitation over the Iberian Peninsula during the last century. J Geophys Res 116:D02109 doi:10.1029/2010JD014255

Goodess C, Jones P (2002) Links between circulation and changes in the characteristics of Iberian rainfall. Int J Climatol 22:1593–1615

Guirguis K, Gershunov A, Schwartz R, Bennett S (2011) Recent warm and cold daily winter temperature extremes in the Northern Hemisphere. Geophys Res Lett 38:L17701 doi:10.1029/2011GL048762

Hess P, Brezowsky H 1952. Katalog der Großwetterlagen Europas (Catalogue of the European large scale weather types). Ber Dt Wetterd in der US-Zone 33, Bad Kissingen

Hidalgo-Muñoz JM, Argüeso D, Gámiz-Fortis SR, Esteban-Parra MJ, Castro-Díez Y (2011) Trends of extreme precipitation and associated synoptic patterns over the southern Iberian Peninsula. J Hydrol (Amst) 409:497–511

Hurrell JW (1995) Decadal trends in the North-Atlantic Oscillation: regional temperatures and precipitation. Science 269:676–679

Huth R, Beck C, Philipp A, Demuzere M and others (2008) Classifications of atmospheric circulation patterns: recent advances and applications. Ann NY Acad Sci 1146: 105–152

Jacobeit J (1993) Regionale Unterschiede im atmosphärischen Zirkulationsgeschehen bei globalen Klimaveränderungen (Regional differences of the atmospheric circulation under conditions of global climate change). Erde 124:63–77

Jacobeit J (2010) Classifications in climate research. Phys Chem Earth 35:411–421

Jacobeit J, Wanner H, Luterbacher J, Beck C, Philipp A, Sturm K (2003) Atmospheric circulation variability in the North Atlantic-European area since the mid-seventeenth century. Clim Dyn 20:341–352

Jacobeit J, Rathmann J, Philipp A, Jones PD (2009) Central European precipitation and temperature extremes in relation to large-scale atmospheric circulation types. Meteorol Z 18:397–410

Jones PD, Lister DH (2009) The influence of the circulation on surface temperature and precipitation patterns over Europe. Clim Past 5:259–267

Jones PD, Osborn T, Briffa KR (2003) Pressure-based measures of the North Atlantic Oscillation (NAO): a comparison and an assessment of changes in the strength of the NAO and in its influence on surface climate parameters. Geophys Monogr 134:51-62

Jung T, Hilmer M, Ruprecht E, Kleppek S, Gulev SK, Zolina O (2003) Characteristics of the recent eastward shift of interannual NAO variability. J Clim 16:3371–3382

Kendall MG (1938) 1938: a new measure of rank correlation. Biometrika 30:81–93

Klein Tank AMG, Wijngaard JB, Können GP, Böhm R (2002) Daily dataset of 20th-century surface air temperature and precipitation series for the European Climate Assessment. Int J Climatol 22:1441–1453

Klok EJ, Klein Tank AMG (2009) Updated and extended European dataset of daily climate observations. Int J Climat 29(8):1182-1191

Kostopoulou E, Jones PD (2005) Assessment of climate extremes in the Eastern Mediterranean. Meteorol Atmos Phys 89:69–85

Küttel M, Luterbacher J, Wanner H (2011) Multidecadal changes in winter circulation-climate relationship in Europe: frequency variations, within-type modifications, and long-term trends. Clim Dyn 36:957–972

Lamb H (1972) British Isles weather types and a register of daily sequence of circulation patterns, 1861–1971. Geophys Mem 116, HMSO, London

Lorenzo MN, Taboada JJ, Gimeno L (2008) Links between circulation weather types and teleconnection patterns and their influence on precipitation patterns in Galicia (NW Spain). Int J Climatol 28:1493–1505

Moberg A, Jones P, Lister D, Walther A and others (2006) Indices for daily temperature and precipitation extremes in Europe analyzed for the period 1901–2000. J Geophys Res 111:D22106

Muñoz-Diaz D, Rodrigo FS (2004) Impacts of the North Atlantic Oscillation on the probability of dry and wet winters in Spain. Clim Res 27:33–43

Nykjaer L (2009) Mediterranean Sea surface warming 1985–2006. Clim Res 39:11–17

Ortiz Beviá MJ, Sánchez Gómez E, Álvarez García FJ (2011) North Atlantic atmospheric regimes and winter extremes in the Iberian Peninsula. Nat Hazard Earth Syst Sci 11: 971–980

Osborn TJ, Jones PD (2000) Air flow influences on local climate: observed United Kingdom climate variations. Atmos Sci Lett 1:62–74

Philipp A, Della-Marta PM, Jacobeit J, Fereday D, Jones P, Moberg A, Wanner H (2007) Long-term variability of daily North Atlantic–European pressure patterns since 1850 classified by simulated annealing clustering. J Clim 20:4065–4095

Philipp A, Bartholy J, Beck C, Erpicum M and others (2010) Cost733cat — a database of weather and circulation type classifications. Phys Chem Earth 35:360–373

Pozo-Vázquez D, Esteban-Parra MJ, Rodrigo FS, Castro-Díez Y (2001) A study on NAO variability and its possible non-linear influences on European surface temperatures. Clim Dyn 17:701–715

Ramos AM, Lorenzo N, Gimeno L (2010) Compatibility between modes of low frequency variability and circulation types: a case study of the North West Iberian Peninsula. J Geophys Res 115:D02113

Ramos AM, Trigo RM, Santo FE (2011) Evolution of extreme temperatures over Portugal: recent changes and future scenarios. Clim Res 48:177–192

Rasilla DF, García-Codron JC, Carracedo V, Diego C (2010) Circulation patterns, wildfire risk and wildfire occurrence in continental Spain. Phys Chem Earth 35:553–560

Rodrigo FS (2010) Changes in the probability of extreme daily precipitation observed from 1951 to 2002 in the Iberian Peninsula. Int J Climatol 30(10):1512–1525

Rodrigo FS, Trigo RM (2007) Trends in daily rainfall in the Iberian Peninsula from 1951 to 2002. Int J Climatol 27: 513–519

Rodrigo FS, Pozo-Vázquez D, Esteban-Parra MJ, Castro-Díez Y (2001) A reconstruction of the winter North Atlantic Oscillation index back to AD 1501 using documentary data in southern Spain. J Geophys Res 106: 14805–14818

Rodríguez-Fonseca B, Rodríguez-Puebla C (2010) Teleconexiones climáticas en el entorno de la Península Ibérica. Predictabilidad y cambios esperados. In: Pérez FF, Boscolo R (eds) Clima en España: pasado, presente y future. Informe de Evaluación del cambio climático regional, Red Temática CLIVAR, Madrid, p 53-68

Rodríguez-Puebla C, Encinas AH, Saenz J (2001) Winter precipitation over the Iberian Peninsula and its relationship to circulation indices. Hydrol Earth Syst Sci 5: 233–244

Rodríguez-Puebla C, Encinas AH, García-Cansado LA, Nieto S (2010) Trends in warm days and cold nights over the Iberian Peninsula: relationships to large-scale variables. Clim Change 100:667–684

Romero R, Summer G, Ramis C, Genovés A (1999) A classification of the atmospheric circulation patterns producing significant daily rainfall in the Spanish Mediterranean area. Int J Climatol 19:765–785

Sánchez-Lorenzo A, Brunetti M, Calbo J, Martin-Vide J (2007) Recent spatial and temporal variability and trends of sunshine duration over the Iberian Peninsula from a homogenized data set. J Geophys Res D 112:D20115

Slonosky VC, Jones PD, Davies TD (2000) Variability of the surface atmospheric circulation over Europe, 1774–1995. Int J Climatol 20:1875–1897

Scaife AA, Folland CK, Alexander LV, Moberg A, Knight JR (2008) European climate extremes and the North Atlantic Oscillation. J Clim 21:72–83

Slonosky VC, Jones PD, Davies TD (2001) Atmospheric circulation and surface temperature in Europe from the 18th century to 1995. Int J Climatol 21:63–75

Solomon S, Qin D, Manning M, Alley RB and others 2007: Technical summary. In: Climate change 2007: the physical science basis. Contribution of Working Group I to the Fourth Assessment Report of the Intergovernmental Panel on Climate Change. Cambridge University Press, Cambridge

STARDEX (Statistical and regional dynamical downscaling of extremes for European regions) (2005) Final report. Available at www.cru.uea.ac.uk/cru/projects/stardex/

Ting M, Kushnir Y, Seager R, Li C (2009) Forced and internal twentieth-century SST trends in the north Atlantic. J Clim 22:1469–1481

Trigo RM, DaCamara CC (2000) Circulation weather types and their impact on the precipitation regime in Portugal. Int J Climatol 20:1559–1581

Trigo IF, Davies TD, Bigg GR (1999) Objective climatology of cyclones in the Mediterranean region. J Clim 12: 1685–1696

Trigo RM, Osborn TJ, Corte-Real JM (2002) The North Atlantic Oscillation influence on Europe: climate impacts and associated physical mechanisms. Clim Res 20:9–17

Ulbrich U, Christoph M (1999) A shift of the NAO and increasing storm track activity over Europe due to anthropogenic greenhouse gas forcing. Clim Dyn 15: 551–559

Vicente-Serrano SM, López-Moreno JI (2008) Nonstationary influence of the North Atlantic Oscillation on European precipitation. J Geophys Res 113:D20120 doi:10.1029/2008JD010382

Vicente-Serrano SM, Begueria S, Lopez-Moreno JI, El Kenawy AM, Angulo-Martinez M (2009) Daily atmospheric circulation events and extreme precipitation risk in northeast Spain: role of the North Atlantic Oscillation, the Western Mediterranean Oscillation, and the Mediterranean Oscillation. J Geophys Res 114(8):D08106

Vicente-Serrano SM, Trigo RM, López-Moreno JI, Liberato MLR and others (2011) Extreme winter precipitation in the Iberian Península in 2010: anomalies, driving mechanisms and future projections. Clim Res 46:51–65

Wilks DS (1995) Statistitical methods in the atmospheric sciences. Academic Press, San Diego, CA

Yiou P, Nogaj M (2004) Extreme climatic events and weather regimes over the North Atlantic: when and where? Geophys Res Lett 31:L07202. doi:10.1029/2003GL019119

Zhang X, Hegerl G, Zwiers FW, Kenyon J (2005) Avoiding inhomogeneities in percentile-based indices of temperature extremes. J Clim 18:1852–1860

Editorial responsibility: Bryson Bates, Wembley, Australia

Submitted: June 1, 2011; Accepted: February 20, 2012
Proofs received from author(s): June 29, 2012